MULLARD LIMITED
Mullard House
Torrington Place
London, W.C.1

VOL. 8 No. 73 OCTOBER 1964

CONTENTS

Rectifier Diode Operation at Kilocycle Frequencies 66–77

Parallel Operation of Silicon Rectifier Diodes 78–88

Mullard Technical Communications

VOLUME 8 NUMBER 73 October 1964

Mullard Technical Communications

VOLUME 8 NUMBER 73 October 1964

Contents

Rectifier Diode Operation at Kilocycle Frequencies *M. Dayal* 66

Parallel Operation of Silicon Rectifier Diodes *G. J. Tobisch* 78

Mullard Technical Communications contains information on the performance or application of Mullard products such as electronic valves and tubes, semiconductor devices, and electrical and magnetic components. It is issued free-of-charge to equipment designers, research organisations, reference libraries, and educational establishments. Bona fide applications to be added to the circulation list should be made under an official letter head to Central Technical Services. Overseas enquiries should be addressed to the local Mullard agent, or to Mullard Overseas Ltd. at Mullard House.

Abstracts, or references to an article, should mention both the source, *Mullard Technical Communications*, and the authors. Requests for republication or translation should be made to the Editor in writing.

The issue of the information contained in this publication does not imply any authority or licence for the utilisation of any patented feature.

'Mullard' is the trade mark of Mullard Limited and is registered in most of the principal countries of the world.

Editor: F. A. Sowan

Assistant Editors: E. G. Evans R. Barrie

Published by

Central Technical Services
Mullard Limited, Mullard House, Torrington Place, London, W.C.1
LANgham 6633

© Mullard Limited, 1964

Made and Printed in England by
WIGHTMAN AND COMPANY LIMITED, 1/3 BRIXTON ROAD, LONDON, S.W.9

Rectifier Diode Operation at Kilocycle Frequencies

M. DAYAL
Mullard Semiconductor Electrical Development Laboratory

When rectifier diodes are operated at frequencies exceeding the usual limit of 400c/s, the dissipation caused by reverse recovery effects can reach significant proportions, and the rectifier junction may be overheated. It is shown how curves giving maximum allowable current and rectification efficiency as functions of operating frequency up to 10kc/s can be derived for square-wave, pulse, and sinewave operation.

INTRODUCTION

Published data sheets on rectifier diodes usually give limiting values that apply for sinusoidal operation at frequencies from 50c/s to 400c/s. The performance of rectifier circuits at these frequencies has already been described (Ref. 1). At higher frequencies, reverse recovery transients contribute considerably to the heating of the rectifier junction. It is therefore necessary to take into account the dissipation caused by these transients so that the operating temperature is kept within safe limits.

This article investigates the reverse recovery phenomenon and its influence on the high-frequency performance of rectifier diodes. The minority carrier storage curves for sinusoidal and square-wave operation are obtained; and it is shown that the minority carrier storage charge for sinusoidal operation can be estimated, if the transient behaviour of the rectifier during square-wave operation is known. From the experimental results the dissipation due to reverse recovery effects is estimated. It is shown how current derating curves can be derived for square-wave, pulse, and sinusoidal operation of diodes at high frequencies. The beneficial effect of improved cooling is demonstrated. The rectification efficiencies are also calculated.

The physical aspects of semiconductor rectifiers are not discussed, since the main object is to look at the rectifier from the circuit point of view. For an understanding of the theory and design of semiconductor devices, appropriate literature should be consulted (Refs. 2, 3, 4).

The work described in this article was performed on BYZ10 diodes. This type was used for experimental convenience. The article should therefore be regarded as a statement of a general problem and of the steps that can be taken to solve it, rather than as an examination of BYZ10 performance at frequencies above the published maximum.

The BYZ10 has been uprated since the completion of the work described. Designers should therefore base their calculations on the current data sheet, and should regard the curves and calculations in this article as illustrative examples.

POWER LOSSES IN RECTIFIER DIODES

The three main sources of rectifier power loss are:

(i) Forward voltage drop V_F when the rectifier is in its conducting state, giving rise to forward loss P_F.

(ii) Leakage current (also termed inverse current or reverse current) when the rectifier is in its blocking state, giving rise to inverse loss P_i.

(iii) Switching transients when the rectifier is switched from one state to the other.

Forward Loss

When the rectifier is in its steady conducting state, there is a small voltage drop across the rectifier junction. The voltage drop increases with increasing current, but is independent of the frequencies considered in this article.

Consider the normal characteristic of forward voltage drop against current. If we draw a tangent from the peak current I_{pk} back to the voltage axis, we can simplify the calculations by using this tangent instead of the actual curve. The forward loss P_F caused by this voltage drop can be calculated by means of the following equation (Ref. 5):

$$P_{F(av)} = V_o I_o + I_{rms}^2 R \qquad \ldots(1)$$

where

I_o = average forward current per rectifier
I_{rms} = rms current per rectifier over the whole cycle
V_o = voltage given by the intercept of the tangent on the voltage axis of the forward characteristic
R = slope of the tangent to the rectifier forward characteristic.

The forward loss and the inverse loss together form the major part of the power loss at low frequencies.

Inverse Loss

When the rectifier is reverse-biased, it is in its high-resistance state, but a small leakage current still flows. The leakage current is sensitive to temperature, and it may double for every 10 to 15 degC rise in temperature.

The power loss due to leakage current is independent of frequency. The inverse loss at any temperature can be calculated from Eq(2) given below (Ref. 5). The dissipation loss calculated by means of this equation gives a slightly higher value than occurs in practice.

$$P_{i(av)} = V_{RWM} \times I_{i(max)} \times \frac{\left(1-\frac{\phi}{2}\right)\cos\frac{\phi}{2} + \frac{1}{\pi}\sin\frac{\phi}{2}}{1+\cos\frac{\phi}{2}} \qquad \ldots(2)$$

where

V_{RWM} = crest working voltage
$I_{i(max)}$ = maximum inverse current corresponding to V_{RWM}
ϕ = conduction angle.

Switching Losses

The switching losses are caused by the forward switching transients and the reverse switching transients. (They are sometimes termed forward recovery transients and reverse recovery transients respectively.)

Forward Switching Transients

When a semiconductor rectifier is switched from the nonconducting state to the conducting state, it does not reach steady-state conditions in the forward direction instantaneously. The minority carriers (holes, in the case of p-n rectifiers) require a finite time to modulate the conductivity of the material in the vicinity of the junction, and thus reduce the resistance of the device to the flow of current in the forward direction. For a given current, the initial voltage developed across the rectifier is therefore higher than it is in the steady state.

The forward switching transient is shown in Fig. 1. The peak value of the forward recovery voltage V_{fr} depends on the rate of rise of the switching current. The

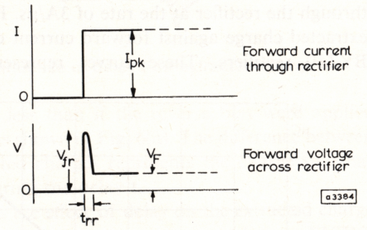

Fig. 1—Forward switching transient

duration of this transient, which is termed the forward recovery time t_{fr}, is generally small compared to the reverse recovery time. The extra dissipation in the device is caused by the forward recovery voltage and the rising forward current. The power loss due to the forward switching transient is normally much smaller than that due to the reverse switching transient, and it may be neglected for most types of rectifier.

Reverse Switching Transients

For a steady-state forward current I_{pk}, there is a corresponding flow of minority carriers from the junction. The minority carriers require a finite time to recombine after the forward voltage is removed, therefore the capability of current flow does not cease instantaneously. The rectifier only attains its high-resistance state in the reverse direction when the minority carriers have recombined within the material.

The process of reverse recovery can be accelerated by applying a reverse bias to the rectifier. If the rate of rise of the switching voltage is high enough, the uncombined minority carriers will be extracted by the reverse voltage in the form of a reverse current spike. The total extracted charge is made up of two components. One component is due to the minority carriers, and the other to the rectifier capacitance, which gives rise to capacitive current in the process of charging.

The idealised form of the reverse recovery transient is shown in Fig. 2. When the rectifier is switched from the forward to the reverse direction, a large transient current I_R can flow owing to the diffusion of the minority carriers back across the junction. This current is limited initially

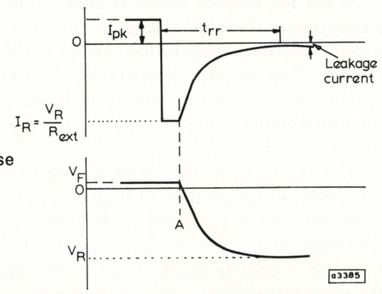

Fig. 2—Reverse switching transient

only by the applied reverse voltage V_R and the external circuit resistance R_{ext}. This condition will prevail, and the rectifier remain forward-biased, until the stored charge concentration at the junction boundary has fallen to zero, at point 'A'. The rectifier resistance then builds up to its high value, and the reverse current decreases to the leakage current value under the normal blocking condition during the reverse recovery period t_{rr}.

The major part of the power loss due to reverse recovery transients occurs while the rectifier resistance is building up to its high value. During this period the voltage across the junction is increasing to the applied reverse voltage V_R, and the peak reverse current I_R is decreasing to the normal leakage current. The reverse transient loss increases with current and frequency. The amount of dissipation caused by this transient is negligible at normal power frequencies; but it can be appreciable at higher frequencies.

REVERSE RECOVERY TRANSIENT MEASUREMENT

The reverse recovery transients obtained in practical circuits differ from the idealised transient shown in Fig. 2. The reverse recovery time, the peak reverse current, and the charge extracted from the rectifier are dependent on a number of circuit parameters, as well as on the rectifier parameters.

For any particular type of rectifier, there will be a spread in the rectifier parameters, therefore there will be a spread in the charge extracted under specified conditions.

The rate of recombination of the minority carriers and the rate of application of the switching voltage are of special importance for estimation of stored charge under pulse conditions. If the switching time is comparable to the recombination time, then the extracted charge will be very different from the initial charge that existed in the device when the switching voltage was applied. The extracted charge will approach the initial charge in the device if the switching time is made much smaller than the recombination time.

The dissipation loss due to the reverse recovery transient will therefore vary with the type of circuit and the circuit conditions for any particular rectifier. It is, however,

useful to know the dissipation due to reverse recovery transients under specified conditions. This information will enable the likely dissipation loss in a particular circuit to be assessed.

SQUARE-WAVE OPERATION AT HIGH FREQUENCIES

When the rectifier which is conducting has reached a steady state, there is always a minority carrier charge present, corresponding to the current flowing through the rectifier. The minority carriers are continuously recombining and new carriers taking their place. The average time of recombination depends on the parameters of the device.

The charge extracted under specified switching conditions will be independent of frequency, provided that the pulse duration is sufficient to allow the rectifier to attain its steady state. The dissipation caused by the reverse transient is directly proportional to the repetition rate of the transient; that is, to the operating frequency.

Reverse Switching Transient Measurement

The reverse recovery transients for various currents have been measured for the condition where the reverse current is equal to the forward current. These values were used in order to establish a standard for measurements. The circuit for measuring the extracted charge is shown in Fig. 3. The thyristor circuit is a conventional cathode

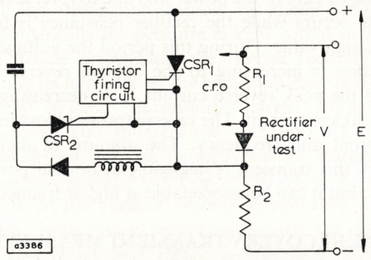

Fig. 3—Measurement of minority carrier charge under pulse conditions

pulse turn-off circuit (Refs. 6, 7). It is used here to apply a switching voltage to reverse-bias the rectifier under test.

The rise-time of CSR_1, which is switched to apply the reverse voltage, must be fast; and the gate pulse applied must be such as to allow CSR_1 to switch on at this rate. Connecting leads should be as short as possible to minimise the inductance in the circuit.

The forward current I_{pk} through the rectifier under test is set by the applied voltage V and the noninductive resistors R_1 and R_2. Thus

$$I_{pk} = \frac{V - V_F}{R_1 + R_2}. \qquad \ldots(3)$$

When CSR_1 is turned on, the applied voltage E should be such that with the rectifier under test short-circuited, the reverse current through resistor R_1 is equal to the forward current I_{pk}. Thus

$$I_R = I_{pk} = \frac{E - E_D - V}{R_1}$$

where

E_D = forward voltage drop across CSR_1

therefore

$$E = V + E_D + I_{pk}R_1. \qquad \ldots(4)$$

Typical current waveforms observed across R_1 are shown in Fig. 4, and the shaded areas represent the extracted charge. At low currents the reverse transient waveform is of the shape shown in Fig. 4(a). It resembles

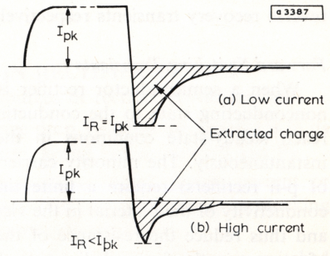

Fig. 4—Current waveforms across R_1

the idealised waveform (Fig. 2). At high currents the rectifier starts to recover before the full reverse current can pass through it, and the shape of the transient is as shown in Fig. 4(b).

The rise-time of CSR_1 was such as to force the current through the rectifier at the rate of 3A/μs. Fig. 5 shows the extracted charge against forward current curves for three BYZ10 rectifiers. These curves represent the typical,

Fig. 5—Extracted charge as a function of peak current for three BYZ10 with minimum, typical, and maximum extracted charge

maximum, and minimum extracted charge measured on some samples available at the time of this investigation. All further considerations in this article are based on the sample from this batch with the maximum extracted charge, since this is the worst condition for high-frequency operation.

For BYZ10 rectifiers, the extracted charge is mainly the charge due to minority carriers, since the rectifier

capacitance is small. The capacitance of a BYZ10 rectifier at 30Mc/s was found to be about 6pF at 400V.

Effect of Delay on Extracted Charge

When a rectifier is switched from a steady forward current I_{pk} to zero current with no reverse bias, the minority carrier charge within the device, corresponding to this peak current, reduces itself by the process of recombination. If, therefore, the reverse bias is applied after a delay t, as shown in Fig. 6(b), then the extracted

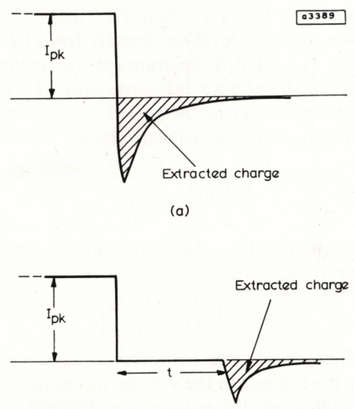

Fig. 6—Influence of delay t on extracted charge

charge will be less than if the reverse bias were applied with no delay as shown in Fig. 6(a). The difference between the two extracted charges represents the charge that has recombined during the delay t.

Fig. 7 shows the effect of delay on the extracted charge for various forward currents, as measured on a BYZ10. The decay is exponential, and the time-constant of the

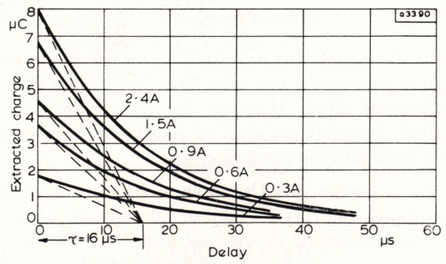

Fig. 7—Extracted charge as a function of delay, for various peak currents

decay ($\tau = 16\mu s$) for all five curves is approximately constant.

An estimate of the initial charge can now be made. If the current through the rectifier reverses at a rate such that it passes through zero current at time t_1 (which is short compared with τ), then during this period the charge is given by the following equation:

$$Q = Q_i e^{-t/\tau} \qquad \ldots(5)$$

where

$t \leqslant t_1$

Q_i = initial charge in the device corresponding to I_{pk}

Q = charge remaining in the device after time t.

As soon as reverse current flows, the process of reduction of charge becomes complex. Part of the charge is being extracted during the period t_{rr}, and at the same time part of the charge is recombining. Fig. 8 shows

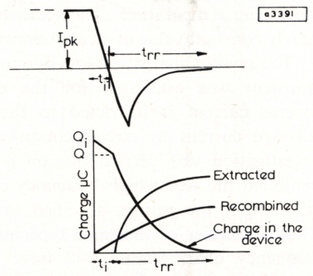

Fig. 8—Actual charge in rectifier

the estimated initial charge Q_i, and the extracted and recombined charges. The estimated initial charge is less than the actual initial charge by the amount that has recombined during the period t_{rr}. Fig. 9 shows the

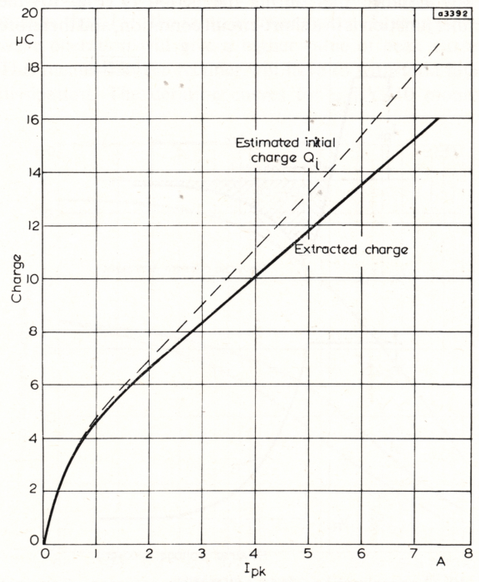

Fig. 9—Extracted charge and estimated initial charge as functions of peak current

extracted charge and the estimated initial charge Q_i against forward current I_{FK} plotted according to Eq(5), for the 'maximum' curve of Fig. 5 and $\tau = 16\mu s$.

Dissipation due to Reverse Switching Transients

The determination of the exact amount of dissipation caused by reverse recovery transients is difficult for a number of reasons. Several parameters of the rectifier are functions of the temperature and geometry of the device. In addition, the amount of charge extracted will depend

on the individual rectifier, the circuit impedance, and the amplitude and rate of the switching voltage. The shape of the switching transient is therefore likely to vary from one rectifier to another, and also from one type of rectifier to another.

For the samples of BYZ10 rectifier investigated, it was observed that the recovery time and the extracted charge under specified conditions ($I_R = I_{pk}$) increased with increasing temperature. The extracted charge reached a nearly constant value at a case temperature above 60°C.

The reverse dissipation loss due to the reverse switching transient was estimated for the condition where the reverse current is restricted to the same value as the forward current by circuit conditions. This part of the investigation was carried out on a BYZ10 sample that exhibited the worst high-frequency characteristic but was still within the ratings specified in the published data. Thus a rectifier of the same type but with a better high-frequency characteristic will have less dissipation loss than that estimated for the worst device.

Estimation of Dissipation

Several assumptions were made in the determination of the dissipation loss due to reverse switching transients. It was assumed that during the period t_2 (Fig. 10) the rectifier junction is in a short-circuit condition, and therefore

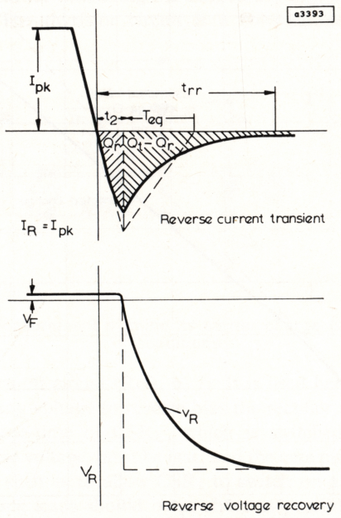

Fig. 10—Approximation for estimating reverse transient dissipation, for square-wave operation

the peak reverse current flowing through the junction at time t_2 is $I_R = I_{pk}$. The dissipation loss during this period is small (since the junction is still forward-biased) compared to the dissipation loss during the remainder of the recovery period.

It was observed from measurements on several samples of BYZ10 that the charge Q_r(Fig. 10) was extracted before the rectifier resistance began to build up rapidly to its high value. The ratio of Q_r to the total charge extracted Q_t, for any one rectifier, remained approximately constant for all values of forward current. The value of this ratio, however, varies from one rectifier to another. For the samples investigated, the spread was from 0·3 to 0·45. The lower value corresponds to the device with the worst high-frequency characteristic and therefore the maximum dissipation.

For the purpose of estimation of the loss, several approximations to the transient waveforms were tried. The following method proved to be the most satisfactory. The approximation for this method is shown in Fig. 10 by broken lines.

Instead of using the experimental peak reverse current, it was assumed that it reached $I_R = I_{pk}$. The reverse current was assumed to decay linearly from $I_R = I_{pk}$ to zero in time T_{eq}. That is, the transient was assumed to be triangular and to enclose the same area as the reverse switching transient during the period $t_{rr}-t_2$. The current waveform can then be defined by the following two equations:

$$\frac{I_R T_{eq}}{2} = Q_t - Q_r. \qquad \ldots(6)$$

During the period T_{eq}, the instantaneous current i_R at time t (where $T_{eq}+t_2 \geqslant t \geqslant t_2$), is given by:

$$i_R = I_R\left(1 - \frac{t-t_2}{T_{eq}}\right). \qquad \ldots(7)$$

The shape of the actual recovery voltage waveform is shown by the full line in the voltage waveform of Fig. 10. As a simplification, the voltage was assumed to rise instantaneously at time t_2 to the peak applied reverse voltage V_R, so that

$$v_R = V_R. \qquad \ldots(8)$$

The dissipation loss W_R at frequency f is given by the following expressions:

$$W_R = f\int_{t_2}^{T_{eq}+t_2} (v_R i_R dt) \qquad \ldots(9)$$

from which

$$W_R = \frac{I_R V_R T_{eq} f}{2}. \qquad \ldots(10)$$

The dissipation loss estimated by means of the above equation gave results that were 20 to 30% higher than the experimental values. However, the error is in the right direction, and therefore gives an added margin of safety.

To generalise the procedure, let

$$Q_r = kQ_t \qquad \ldots(11)$$

From Eqs(6) and (11)

$$W_R = (1-k)Q_t V_R f. \qquad \ldots(12)$$

For the devices investigated, the lowest value of k determined was 0·3. Making allowances for temperature variation and so on, let k = 0·2. Then

$$W_R = 0{\cdot}8 Q_t V_R f. \qquad \ldots(13)$$

Curves for W_R against frequency for a fixed voltage of V_R = 100V and for various values of forward current, are shown in Fig. 11. The value of $Q_t = Q_i$ obtained from Fig. 9 was used.

This graph has been drawn for $I_R = I_{pk}$; but it is also applicable for any value of I_R, because Q_t remains unaltered.

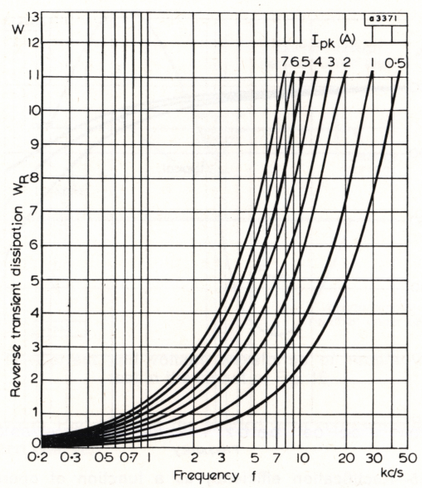

Fig. 11—Dissipation as a function of operating frequency, for reverse voltage V_R of 100V, at various peak currents. For dissipation at any other reverse voltage V_{R1}, multiply the value read off by $V_{R1}/100$.

Derating of Rectifiers

It is seen from Eq(13) that the dissipation loss of the rectifier due to reverse switching transients increases with frequency. If the frequency is high enough, these losses are substantial and must be taken into account. Either the cooling facilities must be improved, or the rectifier current must be derated to ensure that the additional dissipation does not damage the rectifier.

Fig. 12 shows the derating curves for square-wave operation up to an ambient temperature of 55°C.

The derating curves of Fig. 12 were derived from the design curves given in the BYZ10 published data extant at the time of the experimental work, and the dissipation loss calculated from Eq(13) or obtained from Fig. 11. The procedure can best be illustrated by an example.

Suppose that a BYZ10 rectifier is mounted on a heatsink with a thermal resistance θ_h of 4·4degC/W. The supply voltage is a 200V (peak to peak) square-wave, and the maximum ambient temperature is 55°C. What is the maximum frequency at which a mean current of 1A can be passed through the rectifier?

From the published data, for an ambient temperature of 55°C, and low-frequency operation

$$\theta_h + \theta_i = 4{\cdot}4 + 0{\cdot}6 = 5\text{degC/W}.$$

The dissipation due to forward voltage drop and leakage current is given by $P_F + P_i = P_{tot(max)}$. From published data $P_{tot(max)}$ = 8·6W. For high-frequency operation at 1A average current $P_{tot(max)}$ = 3·1W, therefore the additional dissipation allowed in the rectifier = 8·6−3·1 = 5·5W.

For a square wave $I_{pk} = 2I_o$ = 2A and V_R = 100V.

From Fig. 9, for I_{pk} = 2A, Q_i = 6·9μC.

Substitution in Eq(10) gives f_{max} = 10kc/s.

It can be seen that if V_R is doubled, f_{max} will be halved.

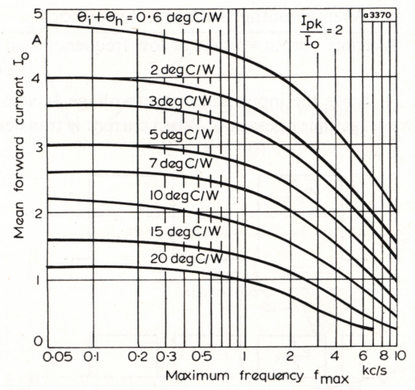

Fig. 12—Current derating for square-wave operation, with reverse voltage V_R of 100V, max ambient temperature of 55°C, and various values of $\theta_i+\theta_h$. For f_{max} at any other reverse voltage V_{R1}, multiply the value read off by $100/V_{R1}$

Pulse Operation at High Frequency

The amount of minority carrier charge present in the rectifier depends on the value of the peak current (Fig. 9). With pulse operation, where the off/on duty cycle ratio is greater than 1:1, the same average current I_o as in square-wave operation will give a higher value of peak current. This means that the rectifier will have to withstand higher dissipation. The derating curves for a BYZ10 mounted

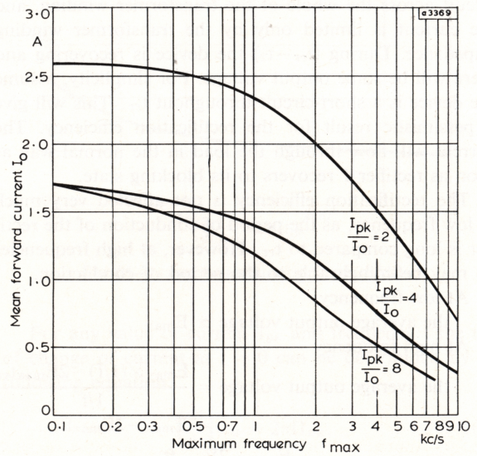
a3369
Mean forward current I_o
A
0 0·5 1·0 1·5 2·0 2·5 3·0
$\frac{I_{pk}}{I_o}$ = 2
$\frac{I_{pk}}{I_o}$ = 4
$\frac{I_{pk}}{I_o}$ = 8
0·1 0·2 0·3 0·5 0·7 1 2 3 4 5 6 7 8 9 10
Maximum frequency f_{max}
kc/s

Fig. 13—Current derating for pulse operation, with reverse voltage V_R of 100V, max ambient temperature of 55°C, and $\theta_i+\theta_h$ = 7degC/W. For f_{max} at any other reverse voltage V_{R1}, multiply the value read off by $100/V_{R1}$

on a heatsink with a thermal resistance giving $\theta_h+\theta_i$ = 7degC/W are shown in Fig. 13 for various values of peak-to-mean current ratio. This thermal resistance is typical of the heatsinks with which the BYZ10 would be used.

Rectification Efficiency

The rectification efficiency η_f is defined as

$$\eta_f = \frac{\text{Average output voltage at frequency f}}{\text{Average output voltage at low frequency } f_{low}}. \quad \ldots(14)$$

Fig. 14 shows the input and output voltage waveforms of full-wave rectifier operation. When current is transferred

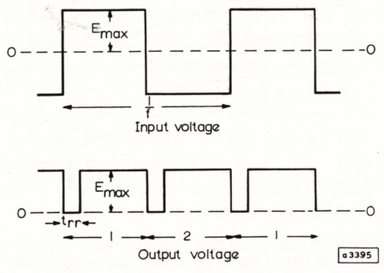

Fig. 14—Influence of recovery time t_{rr} on rectification efficiency, in the full-wave rectifier circuit shown

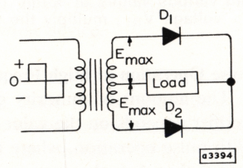

from rectifier 1 to rectifier 2 at the end of the half cycle, rectifier 1 presents a low-impedance path during the time t_2 ; therefore during this period there is virtually a short-circuit across the whole of the transformer winding, and the current is limited only by the transformer winding impedance. During $(t_{rr}-t_2)$ the device is recovering and there will be some output voltage. For simplicity, assume the device is a short-circuit throughout t_{rr}. This will give a pessimistic result for the rectification efficiency. The current will flow through the load in the normal way as soon as rectifier 1 recovers to its blocking state.

The rectification efficiency is not affected very much at low frequency, as the period of conduction of the rectifier is long compared to t_{rr}. However, at high frequencies t_{rr} may be comparable to the period of conduction.

At low frequency

the average output voltage $\simeq E_{max}$

At high frequency

$$\text{the average output voltage} = \frac{E_{max}\times(1/f)-2E_{max}t_{rr}}{1/f}$$
$$= E_{max}-2E_{max}ft_{rr}.$$

$$\eta_f = \frac{E_{max}-2E_{max}ft_{rr}}{E_{max}} \quad \ldots(15)$$

therefore

$$\eta_f\% = (1-2ft_{rr})\times 100. \quad \ldots(16)$$

The above expression indicates that η_f is directly dependent on the recovery time t_{rr}. Since t_{rr} varies from one rectifier to another, the rectification efficiency will vary from one diode to another. Fig. 15 shows rectification efficiency curves for three samples of BYZ10, having t_{rr} values of 25, 17, and 12μs. These curves apply for $I_R = I_{pk}$. If I_R is greater than I_{pk} , then t_{rr} reduces exponentially, and the rectification efficiency is improved.

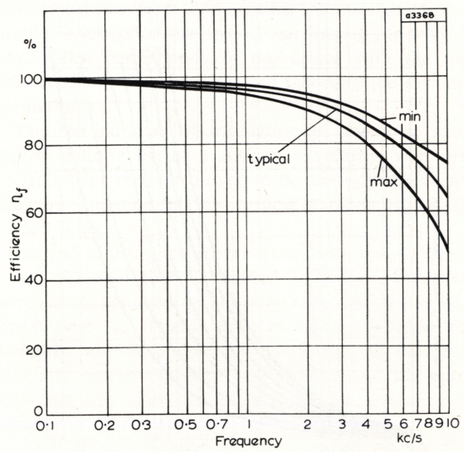

Fig. 15—Rectification efficiency as a function of operating frequency, for square-wave operation. The curves are for the rectifiers with minimum, typical, and maximum extracted charge (see Fig. 5)

SINUSOIDAL OPERATION AT HIGH FREQUENCIES

In square-wave operation the charge in the device corresponding to any forward current I_{pk} is independent of frequency. In sinusoidal operation the charge in the device varies not only with peak current but also with frequency. It is shown on page 76 that an approximate relationship can be established between the two forms of operation.

Reverse Switching Transient Measurement

The circuit used for the measurement of the minority carrier charge in a rectifier under sinusoidal operation is shown in Fig. 16. Rectifier A is the device under test and

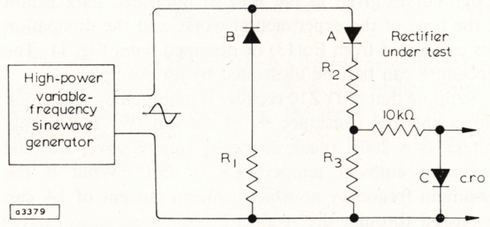

Fig. 16—Measurement of minority carrier charge under sinusoidal conditions

rectifier B is used to present a balanced load to the high-power variable-frequency generator. A fast switching diode C with high back resistance is used to cut off the positive half cycle of the voltage waveform that appears across R_3 , so as not to overload the oscilloscope amplifier when measuring the reverse switching transient.

The extracted charge was measured for the condition where the maximum possible reverse current I_R that can flow through the rectifier is limited to a value equal to the peak forward current I_{pk}. The waveforms across R_3 are

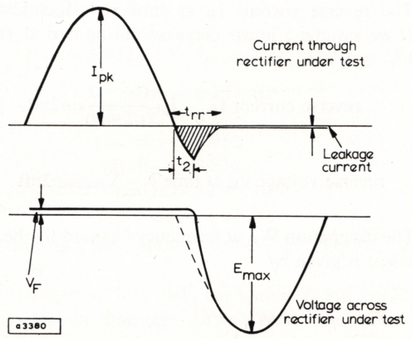

Fig. 17—Current and voltage waveforms of rectifier under test in the circuit of Fig. 16

shown in Fig. 17, and the shaded area represents the extracted charge.

Experimental Results

Fig. 18 shows curves of extracted charge against current I_{pk} for various frequencies. These curves are plotted for a BYZ10 rectifier that exhibited the worst

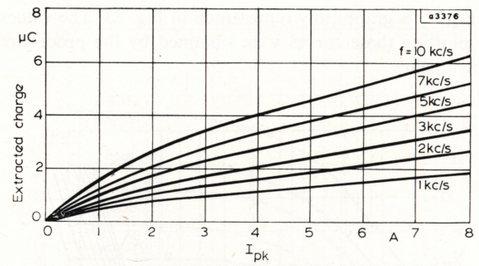

Fig. 18—Extracted charge as a function of peak current for sinewave operation at various frequencies

high-frequency characteristic. The charge will vary from rectifier to rectifier because of the spread in the internal parameters of the rectifiers. It is seen that the amount of charge extracted increases with increasing current and frequency. From these experimental results it was observed that for any fixed peak current I_{pk} , the extracted charges at frequencies f_1 and f_2 for any particular rectifier are related by the following expression:

$$Q_{f2} \simeq Q_{f1}\sqrt{(f_2/f_1)}. \quad \ldots(17)$$

It was further observed that if the current at which the charge is measured is halved and the frequency at which the charge is measured is doubled, then in the two cases the extracted charge is approximately the same. Fig. 19 shows the transient waveforms for $I_{pk} = 6{\cdot}3A$, f = 5kc/s, and also for $I_{pk} = 3{\cdot}14A$, f = 10kc/s. The shapes of the transients, and the extracted charges, are approximately the same. The only common factor between the two operations is the rate of change of current at $t = 0, \pi, 2\pi \ldots .$

Thus

$$Q_{f2} \simeq Q_{f1} \quad \ldots(18)$$

when

$$I_{pk1}/2 = I_{pk2} \text{ and } 2f_1 = f_2.$$

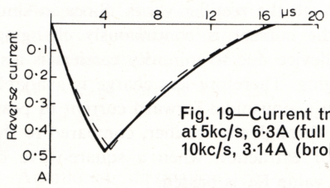

Fig. 19—Current transients at 5kc/s, 6·3A (full line) and 10kc/s, 3·14A (broken line)

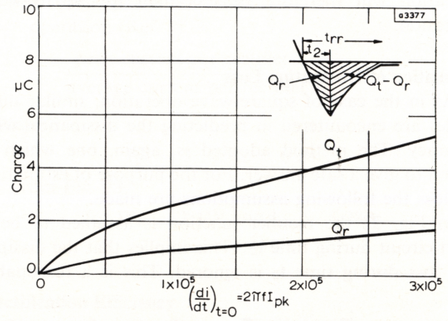

Fig. 20—Extracted charge as a function of $(di/dt)_{t=0}$

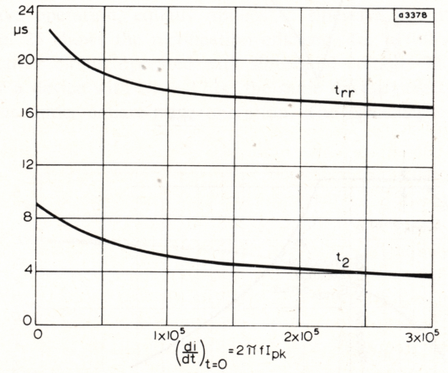

Fig. 21—t_2 and t_{rr} as functions of $(di/dt)_{t=0}$

For any value of current I_{pk} and frequency f the rate of change of current at t = 0 can be determined by the following equation.

$$\left(\frac{di}{dt}\right)_{t=0} = 2\pi f I_{pk}. \quad \ldots(19)$$

Fig. 20 shows the variation in Q_t and Q_r with $(di/dt)_{t=0}$, and Fig. 21 the variation in t_2 and t_{rr} with $(di/dt)_{t=0}$, where Q_t is the total charge extracted during the recovery time t_{rr} , and Q_r is the amount of charge extracted during the period t_2 before the rectifier resistance builds up rapidly to its high value. All four of the above parameters will vary from rectifier to rectifier.

Dissipation Due to Reverse Switching Transients

The minority carriers constitute the mechanism by which the forward current is conducted through the rectifier. The concentration of the minority carriers will vary

as the current through the rectifier varies. Since in sinusoidal operation the current is continuously changing, the charge in the device due to minority carriers is also continuously changing. Therefore less charge is available for extraction when a sinusoidal forward current of peak value I_{pk} is passed through the rectifier, compared to the charge available for extraction when a square-wave of forward current of value I_{pk} is passed.

The dissipation caused by the transient under sinusoidal operation will therefore be less than for square-wave operation.

Estimation of Dissipation Loss

As in the case of square-wave operation, similar difficulties are encountered in predicting the dissipation with accuracy. The method adopted is, again, one which is bound to give a safe answer. For the purpose of estimating the loss the following assumptions are made.

In Fig. 22 the rectifier junction is assumed to be a short-circuit during time t_2. This implies that the dissipation loss during time t_2 is ignored. This is a reasonable

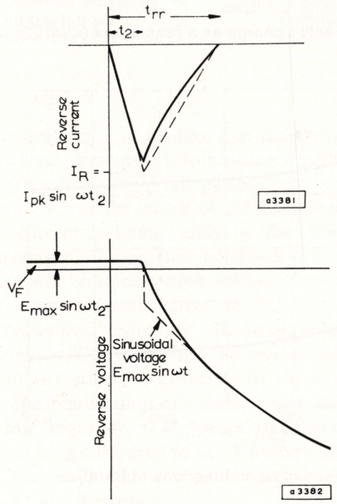

Fig. 22—Approximation for estimating reverse transient dissipation, for sinewave operation

assumption, since the dissipation loss during this time is small compared to the total reverse dissipation loss and therefore may be neglected. Further, the reverse voltage is assumed to rise instantaneously to the value of the applied sine voltage at time t_2, and then to follow the applied voltage. The current is assumed to decrease linearly from I_R to zero in a time $t_{rr}-t_2$. The approximations are indicated in Fig. 22 by broken lines.

Suppose that the applied voltage is $v = V_{max}\sin 2\pi ft$, and the forward current through the rectifier is $i = I_{pk}\sin 2\pi ft$.

The values of t_2 and t_{rr} can therefore be obtained from Fig. 21, using the value of $(di/dt)_{t=0}$ determined from Eq(19).

The reverse current I_R at time $t_2 = I_{pk}\sin 2\pi ft_2$.

If we assume a linear decrease during period $(t_{rr}-t_2)$, and $t_{rr} \geqslant t \geqslant t_2$, then

$$\text{reverse current } i_R = I_{pk}\frac{(t_{rr}-t)}{(t_{rr}-t_2)}\sin 2\pi ft_2 \quad \ldots(20)$$

and

$$\text{reverse voltage } v_R \text{ at time } t = V_{max}\sin 2\pi ft. \quad \ldots(21)$$

The dissipation W_R at frequency f caused by the reverse transient is given by

$$W_R = f\int_{t_2}^{t_{rr}} i_R v_R dt.$$

Substituting for i_R and V_R from Eqs 20 and 21 gives

$$W_R = \frac{fV_{max}I_{pk}\sin 2\pi ft_2}{t_{rr}-t_2}\int_{t_2}^{t_{rr}}(t_{rr}-t)\sin 2\pi ftdt$$

hence

$$W_R = fV_{max}I_{pk}\sin 2\pi ft_2\left[\frac{\cos 2\pi ft_2}{2\pi f} - \frac{\sin 2\pi ft_{rr}-\sin 2\pi ft_2}{(2\pi f)^2(t_{rr}-t_2)}\right]. \quad \ldots(22)$$

Eq(22) is graphically represented in Fig. 23. The values for plotting these curves were obtained by the procedure shown below.

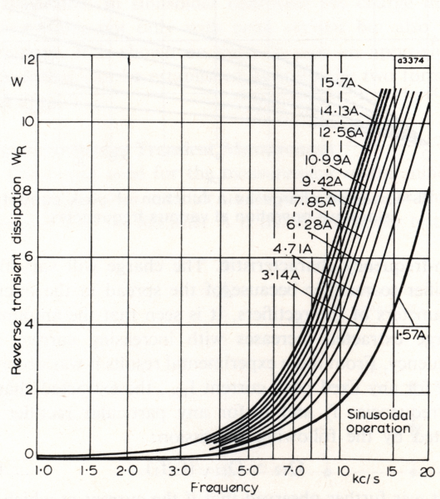

Fig. 23—Dissipation as a function of operating frequency, for reverse voltage V_R of 100V, at various peak currents. For dissipation at any other reverse voltage V_{R1}, multiply the value read off by $V_{R1}/100$

Suppose it is required to determine W_R for a rectifier conducting a sinusoidal forward current of peak value $I_{pk} = 3{\cdot}14$A at 10kc/s, and peak applied voltage = 100V.

From Eq(19)

$$\left(\frac{di}{dt}\right)_{t=0} = 2\pi 10^4 \times 3{\cdot}14 = 1{\cdot}975\times 10^5.$$

From Fig. 21,

for $\left(\frac{di}{dt}\right)_{t=0} = 1{\cdot}975\times 10^5$, $t_{rr} = 17\mu s$, and $t_2 = 4{\cdot}4\mu s$

$$2\pi f = 6{\cdot}28\times 10^4$$
$$\sin 2\pi ft_2 = 0{\cdot}272$$
$$\cos 2\pi ft_2 = 0{\cdot}962$$
$$\sin \pi ft_{rr} = 0{\cdot}876$$
$$(2\pi f)^2 = 39{\cdot}4\times 10^8$$
$$t_{rr}-t_2 = 12{\cdot}6\times 10^{-6}$$

Substituting the above values in Eq(22) gives $W_R = 2{\cdot}8$W.

The dissipation loss W_R calculated from Eq(22) is generally higher than the actual loss. The difference between the estimated loss and the actual loss will depend on how close the actual recovery voltage approached the assumed path of voltage recovery.

Derating of Rectifiers

The dissipation loss W_R estimated in the previous section must be taken into account when operating rectifiers at frequencies at which this loss is significant. Fig. 24 shows the derating curves drawn for sinewave operation up to an ambient temperature of 55°C. The

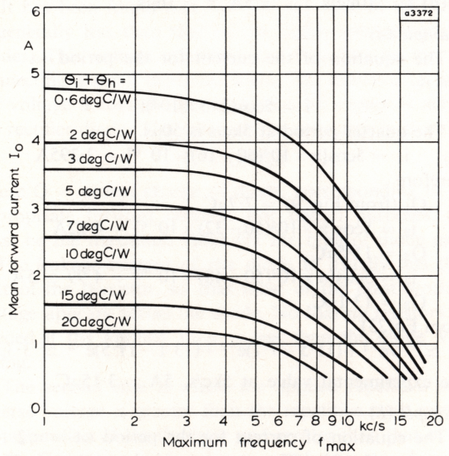

Fig. 24—Current derating for sinewave operation, with reverse voltage V_R of 100V, max ambient temperature of 55°C, and various values of $\theta_i+\theta_h$. For f_{max} at any other reverse voltage V_{R1}, multiply the value read off by $100/V_{R1}$

procedure adopted for deriving these curves is illustrated below by an example.

Suppose that a BYZ10 rectifier is mounted on a heat-sink with a thermal resistance θ_h of 4·4degC/W, giving $\theta_i+\theta_h$ = 5degC/W. It is required to determine the maximum frequency at which a mean current of 2A can be safely passed through the rectifier. The supply voltage is 100V peak, and the maximum ambient temperature is 55°C.

From the published data, for an ambient temperature of 55°C, and low-frequency operation

$$\theta_h+\theta_i = 5\text{degC/W}.$$

Dissipation $P_{tot(max)}$ due to forward voltage drop and leakage current = 8·6W

At average current I_o = 2A, $P_{tot(max)}$ = 5·5W

therefore

Additional dissipation permissible = 8·6−5·5 = 3·1W.

For single-phase sinusoidal operation (Ref. 1)

$$\frac{\text{peak current per rectifier } I_{pk}}{\text{average current per rectifier } I_o} = 3{\cdot}14$$

therefore

$$I_{pk} = 3{\cdot}14\times 2 = 6{\cdot}28\text{A}.$$

From Fig. 23,

for W_R = 3·1W and I_{pk} = 6·28A
f_{max} = 8·8kc/s.

Rectification Efficiency

The rectification efficiency η_f is dependent on the reverse recovery time t_{rr} as in the case of square-wave operation. Eq(16), derived for the efficiency under square-wave operation, equally applies to sinewave operation. Fig. 25 shows the rectification efficiency for a full-wave rectifier circuit operated with sinusoidal voltage. This is for a device with $t_{rr} = 17\mu s$; the same device gave $t_{rr} = 25\mu s$ under square-wave operation. The efficiency curve

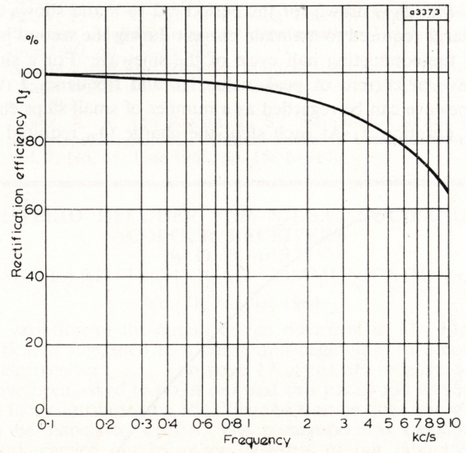

Fig. 25—Rectification efficiency as a function of operating frequency, for sinewave operation

shown will vary slightly with current, since, at any given frequency, t_{rr} will tend to decrease with increasing peak current (Fig. 21).

The rectification efficiency for sinusoidal operation is higher than that for square-wave operation. This is because $t_{rr(sinewave)}$ is less than $t_{rr(square\text{-}wave)}$.

RELATIONSHIP BETWEEN CHARGE EXTRACTED IN SQUARE-WAVE AND SINEWAVE OPERATION

The concentration of the minority carriers in the rectifier at any instant is largely dependent on the current flowing through the rectifier at that instant. In square-wave operation, when the rectifier is switched to the forward conducting state the concentration of minority carriers reaches a steady state once the forward current is established. In sinewave operation the amplitude of the forward current is continuously changing, therefore the concentration of the minority carriers will tend to vary continuously. The concentration increases as the forward current increases to its peak value, and then tends to decrease as the current reduces to zero. The charge in the device during this period can reduce only at the rate allowed by the decay time-constant τ.

It is shown below that if we know both the extracted-charge/peak-current relationship of a rectifier under square-wave operation (Fig. 9), and the time-constant τ (Fig. 7), then the charge extracted for a sinewave of current with a peak value I_{pk} and frequency f, can be estimated.

Estimation of Charge

Consider a rectifier which is passing a forward current that varies sinusoidally. Since the rate of change of current in the region of the peak current is small, it is reasonable to assume that the charge corresponding to the peak current is established in the rectifier at $\omega t = \pi/2$. It therefore follows that any excess charge present in the device when the current falls to zero, occurs during the period $\omega t = \pi/2$ to $\omega t = \pi$.

Fig. 26 is drawn for the period $\pi/2$ to π and shows the charge required to maintain current during the second half of the conducting half cycle of the sinewave. For a sinewave of current of peak value I_{pk} and frequency f, the sinewave can be regarded as a number of small steps each of duration τ. At each step, the charge Q_m required to maintain current can be plotted against time as shown in Fig. 26, using the value of $Q_m = Q_i$ obtained from Fig. 9.

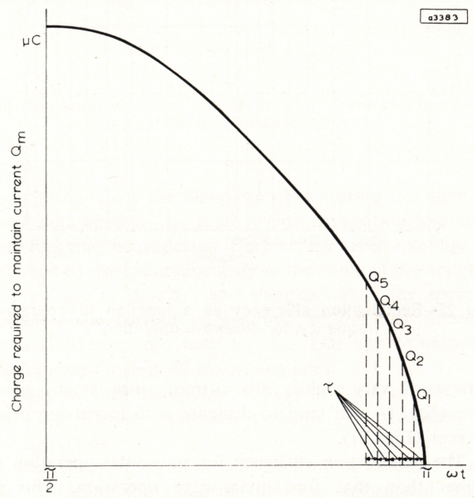

Fig. 26—Charge required to maintain current

In the interval τ just before the current reaches zero, a charge Q_1 is required to maintain current. This charge will reduce to Q_1e^{-1} when the current passes through zero. In the next interval τ, the excess charge is Q_2-Q_1. and this charge reduces to $(Q_2-Q_1)e^{-2}$ when the current passes through zero. The charge Q_e extracted from the rectifier under sinusoidal operation can therefore be expressed approximately by the following series.

$$Q_e \simeq Q_1e^{-1}+(Q_2-Q_1)e^{-2}+(Q_3-Q_2)e^{-3}+(Q_4-Q_3)e^{-4}+(Q_5-Q_4)e^{-5}\ldots \quad \ldots(23)$$

In deriving the above expression it is assumed that the charge that is recombined during the reverse recovery period t_{rr} under sinusoidal operation is the same as that under square-wave operation.

Comparison of Estimated and Experimental Results

The estimated and experimental results are given in Table 1. There is fair agreement between the results. The examples below illustrate the method of deriving these figures.

It is required to estimate the charge extracted under sinusoidal operation at

(a) f = 5kc/s, I_{pk} = 5A, $\tau = 16\mu s$

(b) f = 10kc/s, I_{pk} = 5A, $\tau = 16\mu s$.

Example (a)

The equation of the current for the period $\omega t = \pi/2$ to π is

$$i = 5\cos(2\pi 5\times 10^3)t.$$

The quarter period at 5kc/s is 50μs.

$$i_1 = 5\cos[\pi\times 10^4(50-16)\times 10^{-6}] = 2{\cdot}395A$$

therefore

Q_1 (from Fig. 9) = 7·7μC

$$i_2 = 5\cos[\pi\times 10^4(50-32)\times 10^{-6}] = 4{\cdot}22A$$

$Q_2 = 11{\cdot}5\mu C$

$$i_3 = 5\cos[\pi\times 10^4(50-48)\times 10^{-6}] = 4{\cdot}99 \simeq 5A$$

$Q_3 = 13{\cdot}1\mu C$.

From Eq(23)

$$Q_e \simeq 7{\cdot}7e^{-1}+(11{\cdot}5-7{\cdot}7)e^{-2}+(13{\cdot}1-11{\cdot}5)e^{-3} \simeq 3{\cdot}3\mu C.$$

The experimental value at 5kc/s, 5A = 3·15μC.

Example (b)

The equation of current for the period $\omega t = \pi/2$ to π is $i = 5\cos(2\pi 10^4)t$. The quarter period at 10kc/s is 25μs.

$$i_1 = 5\cos[2\pi 10^4(25-16)\times 10^{-6}] = 4{\cdot}22A$$

$$Q_1 = 11{\cdot}5\mu C$$

i_2 must be taken as I_{pk} = 5A, since $2\tau > 25\mu s$ therefore $Q_2 = 13{\cdot}1\mu C$.

From Eq(23)

$$Q_e = 11{\cdot}5e^{-1}+(13{\cdot}1-11{\cdot}5)e^{-\frac{25}{16}} \simeq 4{\cdot}56\mu C.$$

The experimental value at 10kc/s, 5A = 4·52μC.

DIODE AND THYRISTOR IN SERIES

Knowledge of the reverse recovery characteristics of rectifier diodes is also of particular interest in thyristor applications (not necessarily high-frequency). Where a rectifier diode is connected in series with a thyristor to protect the thyristor against reverse breakdown, the extra components to be used depend on the voltages present.

TABLE 1: Comparison of Estimated Charge Q_{est} and Measured Charge Q_{exp}

The values are in micro-coulombs

I_{pk} (A)	f = 10kc/s		f = 7kc/s		f = 5kc/s		f = 3kc/s		f = 2kc/s		f = 1kc/s	
	Q_{est}	Q_{exp}	Q_{est}	Q_{exp}	Q_{est}	Q_{exp}	Q_{est}	Q_{exp}	Q_{est}	Q_{exp}	Q_{est}	Q_{exp}
0·5	1·11	0·90	0·96	0·70	0·84	0·40	0·59	0·42	0·46	0·30	0·26	0·26
1·0	1·64	1·60	1·49	1·22	1·30	1·00	1·01	0·80	0·78	0·60	0·47	0·45
2·0	2·45	2·60	2·20	2·10	1·96	1·70	1·55	1·30	1·26	1·05	0·79	0·77
3·0	3·15	3·40	2·81	2·80	2·45	2·30	1·98	1·72	1·59	1·35	1·05	0·95
4·0	3·85	4·00	3·38	3·35	2·92	2·75	2·34	2·10	1·87	1·60	1·27	1·12
5·0	4·56	4·52	3·96	3·80	3·36	3·15	2·68	2·40	2·14	1·90	1·43	1·30
6·0	5·32	5·10	4·59	4·25	3·77	3·60	2·99	2·75	2·39	2·15	1·62	1·48
7·0	6·06	5·60	5·15	4·70	4·39	4·00	3·32	3·10	2·65	2·40	1·78	1·62

The first case to be considered is where the applied repetitive peak reverse voltage V_{RR} is greater than the repetitive peak reverse voltage rating of the thyristor, but less than that of the diode. The rectifier diode must then recover before the voltage across the thyristor has risen to the thyristor's repetitive peak reverse voltage rating.

It has been found that the recovery time of thyristors is generally less than that of the higher-voltage rectifier diodes. This voltage condition can therefore be met by connecting a small capacitor across the thyristor to limit the voltage across the thyristor, but no capacitor across the rectifier diode. The value of the capacitor is given by

$$C \geqslant Q/V_{RR} \quad \ldots(24)$$

where Q = stored charge of diode, corresponding to the appropriate forward current. For design purposes, this must be the maximum value for the type of diode used.

The leakage current of the diode is usually less than that of the thyristor, so that most of the crest working voltage appears across the diode. No sharing resistors are needed if the applied V_{RW} is less than the diode V_{RW} rating.

The second case is where the applied repetitive peak reverse voltage is greater than the repetitive peak reverse voltage rating of the thyristor and greater than that of the diode. Capacitors and resistors are thus required across both the thyristor and the diode, as described in Ref. 1.

CONCLUSIONS

From this article it can be concluded that the performance of rectifier diodes at higher frequencies is limited by the dissipation caused by reverse switching transients. This dissipation is greater for pulse and square-wave operation than for sinewave operation.

The rectification efficiency of the rectifiers is directly dependent on the reverse recovery time t_{rr}. Therefore for satisfactory operation at high frequencies both t_{rr} and the extracted charge should be kept to a minimum. Then both the rectification efficiency and the maximum allowable frequency limit will show improvement.

The reverse dissipation under specified conditions varies from diode to diode of any one type. It is thus necessary to know the reverse dissipation and maximum frequency limit for the worst rectifier (from the high-frequency performance point of view) within the specification of any particular type of rectifier.

REFERENCES

1. DAYAL, M. 'Power Rectification with Silicon Diodes'. **Mullard Technical Communications,** Vol. 7, No. 68, Jan 1964, pp. 230 to 262.
2. LE CAN, C. 'Transient Behaviour and Fundamental Transistor Parameters'. **Electronic Applications,** Vol. 20, No. 2, 1959/60, pp. 56 to 83.
3. GAERTNER, W. W. 'Transistors: Principles, Design and Applications'. D. van Nostrand, 1960.
4. JONSCHER, A. K. 'Principles of Semiconductor Device Operation'. G. Bell, 1960.
5. TULEY, J. H. 'Design of Cooling Fins for Silicon Power Rectifiers'. **Mullard Technical Communications,** Vol. 5, No. 44, June 1960, pp. 118 to 130.
6. 'Silicon Controlled Rectifier Manual', Chapter 5: Turn-off Characteristics and Methods. General Electric (U.S.A.) 2nd ed., 1961.
7. PAYNE, R. A. and REEVES, E. S., 'Switch-off Circuits for SCRs Operating on d.c.' **Mullard Technical Communications,** Vol. 7, No. 65, June 1963, pp. 158 to 161.

HYBRID DECODER FOR N.T.S.C. EQUIBAND COLOUR RECEIVERS

by D. R. BIRT

MULLARD TECHNICAL COMMUNICATIONS,

No. 71, August 1964.

A variation of the circuit design described in Mr. Birt's article is suggested in a paragraph beginning 'In a complete receiver . . . . ' on page 17 of the above issue. We have been asked to point out that this paragraph was not in fact contributed by Mr. Birt and that he does not wish to be associated with it. The paragraph was based on work carried out by other members of our laboratory staff, after Mr. Birt had left the employment of the Company. We regret that a contrary impression was given.

SIMPLE THERMOMETER FOR HEATSINK TEMPERATURE MEASUREMENT

MULLARD TECHNICAL COMMUNICATIONS,

No. 72, September 1964.

The instrument described was designed primarily for the measurement of heatsink temperatures in receivers.

When it is used for measuring temperatures of vertical cooling fins in power installations, convection currents may cool the thermistor, and a significantly low reading may be obtained.

Parallel Operation of Silicon Rectifier Diodes

G. J. TOBISCH
Philips Semiconductor Applications Laboratory, Nijmegen

When rectifier diodes are connected in parallel to allow higher powers to be handled, or to increase the reliability of the installation, the differing characteristics of the diodes will lead to unequal current-sharing and to possible overrunning, and destruction of one or more diodes. Preventive measures include operation at an average current per diode that is less than the current rating of the diode. A derating to 0·8+(0·2/n) of the published nominal current is generally satisfactory, where n is the number of diodes in parallel.

Alternative or supplementary measures are selection of diodes for minimum current spread, temperature derating by means of a larger heatsink or increased air-cooling, mounting of the diodes on a shared heatsink, inclusion of series resistors, and the use of balancing transformers.

The relative virtues of these measures are discussed, and the calculations required for the determination of series resistor values, and so on, are included.

INTRODUCTION

Rectifier diodes are connected in parallel for one or both of the following reasons:

(i) to allow higher powers to be handled,

(ii) to improve the reliability of the installation.

There is an inevitable spread in the characteristics of any type of rectifier diode, since it is impossible to manufacture large numbers of devices with absolutely identical characteristics. It is therefore almost certain that, when two or more rectifier diodes are connected in parallel, the conducting paths which they present will differ from one another to a greater or less degree. Thus there will be an unequal division of the current flow through the parallel paths; and it will be possible for the maximum current or temperature ratings to be exceeded by one or more of the diodes.

The present article examines the incidence and magnitude of the differences in the characteristics of the BYZ14, a 40A silicon rectifier diode, and the consequent unequal sharing of current in parallel-diode circuits. The discussion and conclusions are applicable to other types of silicon rectifier diode.

There are a number of methods of promoting a more equal sharing of current. The efficacy of the various methods, and of combinations of methods, is discussed.

GENERAL CONSIDERATIONS

If the forward characteristics of a considerable number of rectifier diodes of some particular type are plotted, it will be found that the curves obtained lie between limiting values, as indicated in Fig. 1. There is a 'spread' on either

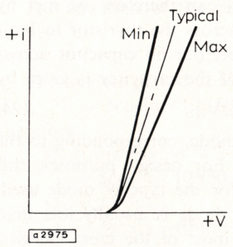

Fig. 1—Spread in BYZ14 characteristics

side of the published nominal characteristic. A histogram, if plotted for a sufficient number of samples, will reveal a distribution, within this spread, of the form shown in Fig. 2 for the BYZ14. There will also be a spread of reverse characteristics.

Spread in Reverse Characteristics

The spread in reverse characteristics is important when rectifier diodes are connected in *series*, because a diode

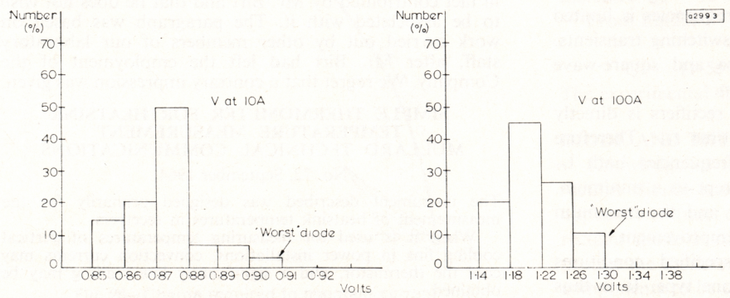

Fig. 2—Histograms of spreads in BYZ14 forward characteristics. The 100A measurements were made under pulse conditions

with a low reverse current will have imposed on it a correspondingly large share of the total voltage drop across the chain (Ref. 1). There is thus a possibility that its peak reverse voltage rating may be exceeded if voltage-sharing elements are not included in the circuit.

In parallel operation, however, differences in the reverse characteristics are of no consequence, since each diode will be clamped to the same reverse voltage; and, if the installation is properly designed, the voltage ratings will not be exceeded. Further, the differences in dissipation are too small to have any marked effect on the temperatures of the diodes.

Spread in Forward Characteristics

It is the spread in the forward characteristic that is of greatest importance in parallel diode operation. Unequal current-sharing can lead to a marked increase in the temperature of diodes that are carrying a disproportionately large share of the total current; and the temperature change will accentuate the characteristic differences. A cumulative process of current and temperature increase may continue to a level at which the maximum current and temperature ratings of the device are exceeded.

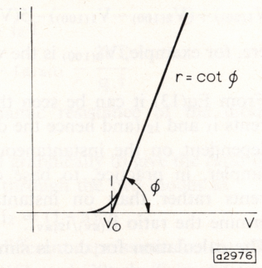

Fig. 3—Idealised forward characteristic of rectifier diode

The forward characteristic of a rectifier diode can be represented, to a first approximation, by the curve shown in Fig. 3, with the formula

$$V = V_o + i.r \qquad \ldots(1)$$

where

V_o = threshold voltage of diode
i = instantaneous current through diode
r = idealised resistance of diode.

In accordance with this formula, the diode can be represented as a battery (with a voltage V_o) in series with a resistance r, as shown in Fig. 4.

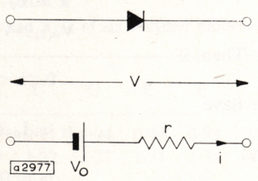

Fig. 4—Equivalent circuit of rectifier diode during forward conduction

The dissipation of the diode is given by

$$W = V_o.i_{av} + i_{rms}^2.r \qquad \ldots(2)$$

where i_{av} and i_{rms} are the average and r.m.s. values of the diode current.

As the forward dissipation increases, the temperature of the diode will also increase, with certain effects on the

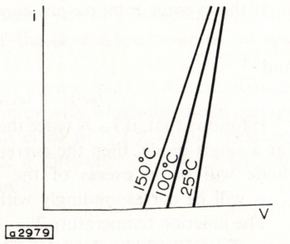

Fig. 5—Forward characteristic as a function of diode temperature

diode forward characteristic. Fig. 5 shows that, with increasing device temperature, the threshold voltage V_o falls and the resistance r rises.

It is worth noting that the maximum operating conditions given in rectifier diode data are determined by the 'worst' diode (that is, the one with the greatest voltage drop V_i at current i), since this diode will have the maximum dissipation. All 'better' diodes would reach maximum dissipation only at currents above the maximum current limit.

CHANGES IN CURRENT AND TEMPERATURE

When two diodes are connected in parallel, it is possible (though not probable) that they will be 'best' and 'worst' diodes; that is, diodes with the lowest and highest allowed values of V_i respectively. However, this least favourable conjunction of diodes will be considered. In most practical cases, two diodes with a smaller difference in characteristics will be used, and the performance will be better than that obtained with opposite-limit samples.

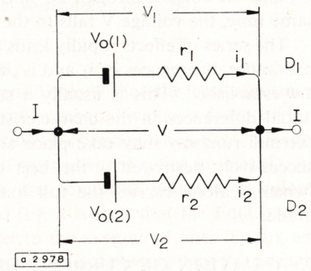

Fig. 6—Equivalent circuit of two parallel diodes during forward conduction

$V_1 = V_2 = V$

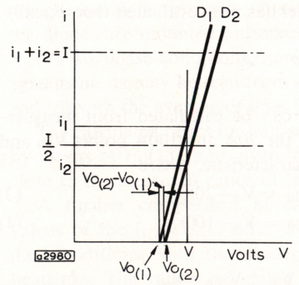

Fig. 7—Forward characteristics of best (D_1) and worst (D_2) diodes in parallel

Fig. 6 represents two diodes in parallel, D_1 being the best diode and D_2 the worst. The forward characteristics of the diodes are shown in Fig. 7, with a current i_1 flowing through the best diode and i_2 through the worst.

If the average total output current is I_{av}, then

$$I_{av} = i_{av(1)} + i_{av(2)}$$

and

$$i_{av(1)} > i_{av(2)}.$$

It follows that, if I_{av} is twice the rated maximum current for a single diode, then the current $i_{av(1)}$ through the best diode will be in excess of the maximum rating, while $i_{av(2)}$ will be correspondingly within the rating.

The junction temperature $T_{j(1)}$ of D_1 will thus be higher than $T_{j(2)}$, and the forward characteristic of D_1 will undergo a greater shift than that of D_2. The effect is illustrated in Fig. 8, where the characteristics of D_1 and D_2 have been shifted by junction temperature changes to the positions indicated by the broken lines D_1' and D_2'. It is seen that the difference in the junction temperature of the two diodes accentuates the unequal sharing of current. Thus, the current through D_1 rises from i_1 to i_1', and the current through D_2 falls from i_2 to i_2'. At the same time, the voltage V falls to the value V'.

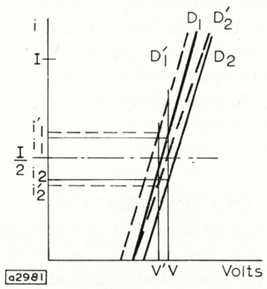

Fig. 8—Effect of temperature on forward characteristic of best (D_1) and worst (D_2) diodes in parallel

The series of effects rapidly leads to a state in which the maximum divergences of i_1 and i_2, and of $T_{j(1)}$ and $T_{j(2)}$, are established. This is usually a stable state; but if the initial differences in the characteristics are great enough, thermal runaway may take place and the diodes may be successively destroyed – the best diode first, and then (when it alone carries the full load current) the worst diode.

EVALUATION OF CURRENT DIFFERENCE

The maximum current difference for two BYZ14 rectifier diodes in parallel has been evaluated theoretically, with Eq(1),

$$V = V_o + i.r.$$

as the starting-point.

Values of V_o and r can be calculated from measurements on the devices at the 20A and 100A points V_{20} and V_{100} on the forward characteristic, where

$$V_{20} = V_o + 20r, \qquad \ldots(3)$$

$$V_{100} = V_o + 100r. \qquad \ldots(4)$$

and (by eliminating r)

$$\frac{V_{20} - V_o}{20} = \frac{V_{100} - V_o}{100}. \qquad \ldots(5)$$

From this equation, the threshold voltage V_o is given by

$$V_o = \frac{100V_{20} - 20V_{100}}{80}. \qquad \ldots(6)$$

Similarly, by eliminating V_o from Eqs(3) and (4),

$$r = \frac{V_{100} - V_{20}}{80}. \qquad \ldots(7)$$

From Fig. 6,

$$V = V_1 = V_2$$

$$= V_{o(1)} + i_1.r_1 \qquad \ldots(8)$$

$$= V_{o(2)} + i_2.r_2 \qquad \ldots(9)$$

and

$$i_1 + i_2 = I, \qquad \ldots(10)$$

where I is the instantaneous total current.

From these equations the following expressions for the diode currents can be obtained:

$$i_1 = \frac{Ir_2 + V_{o2} - V_{o1}}{r_1 + r_2} \qquad \ldots(11)$$

$$i_2 = \frac{Ir_1 + V_{o1} - V_{o2}}{r_1 + r_2} \qquad \ldots(12)$$

It can now be shown that the ratio of instantaneous currents through the rectifiers D_1 and D_2 is given by

$$\frac{i_1}{i_2} = \frac{\frac{I}{20}(V_{2(100)} - V_{2(20)}) - (V_{2(100)} - V_{1(100)}) + 5(V_{2(20)} - V_{1(20)})}{\frac{I}{20}(V_{1(100)} - V_{1(20)}) + (V_{2(100)} - V_{1(100)}) - 5(V_{2(20)} - V_{1(20)})} \qquad \ldots(13)$$

where, for example, $V_{2(100)}$ is the value of V_{100} for rectifier D_2.

From Eq(13) it can be seen that the ratio of the two currents i_1 and i_2 (and hence the difference between them) is dependent on the instantaneous value I. However, it is simpler, in practice, to base calculations on average currents rather than on instantaneous values, and to determine the ratio $i_{1(av)}/i_{2(av)}$.

The calculation for d.c. is simple, since the values of instantaneous, average, r.m.s., and peak current are identical. In a six-phase system also, this is substantially true; but in half-wave systems the ratio $i_{1(av)}/i_{2(av)}$ can be obtained only by integration.

In any positive half-cycle, the best diode D_1, with the lower value of threshold voltage, will start to conduct before the worst diode D_2. Let the difference in time correspond to the interval α, and let x be the conduction angle. Then, for an applied voltage $V_{max}\sin x$,

$$V_{o(1)} = V_{max}\sin x_1$$

$$V_{o(2)} = V_{max}\sin x_2.$$

Therefore

$$\alpha = x_2 - x_1$$

if

$$V_{o(2)} > V_{o(1)}.$$

Then, if

$$0 < x < \alpha$$

we have

$$i_1 = I_{pk}\sin x \qquad \ldots(14)$$

and

$$i_2 = 0. \qquad \ldots(15)$$

Or, if

$$\alpha < x < \frac{\pi}{2}$$

then from Eqs(11) and (12) we have

$$i_1 = \frac{I_{pk}\sin x.r_2 + V_{o(2)} - V_{o(1)}}{r_1 + r_2} \qquad \ldots(16)$$

and

$$i_2 = \frac{I_{pk}\sin x.r_1 + V_{o(1)} - V_{o(2)}}{r_1 + r_2}. \qquad \ldots(17)$$

where r_1 and r_2 are the idealised resistances of D_1 and D_2.

It can be shown that

$$\frac{i_{1(av)}}{i_{2(av)}} = \frac{1 + (r_2/r_1)}{\cos\alpha - \sin\alpha\left(\frac{\pi}{2} - \alpha\right)} - 1 \qquad \ldots(18)$$

where

$$\sin\alpha = \frac{V_{o(2)} - V_{o(1)}}{I_{pk}.r_1}.$$

The forward characteristic of a rectifier diode can also be represented (Ref. 2) by

$$i = i_o.\exp(qV_o/2kT)$$

where k = Boltzmann's constant, T = junction temperature in °K, and q = charge of an electron. Then, for two diodes in parallel,

$$r_1 - \frac{V_{2(100)} - V_{1(100)} - 100(r_2 - r_1)}{I} - a(r_1 + r_2) = \frac{2kT}{qI}\ln\frac{a}{1-a} \qquad \ldots(19)$$

where

$$a = i_2/I$$

$$r = r_{dyn(i)} - \frac{2kT}{q.i}$$

and $r_{dyn(i)}$ is the dynamic resistance of the diode at current i.

Eq(19) can be solved graphically to give the ratio of the instantaneous currents through the two diodes as

$$i_1/i_2 = (1-a)/a. \qquad \ldots(20)$$

We now have three different expressions for the current ratio, namely Eqs(13), (18), and (20). In Table 1 (page 88) lines (a) to (e) are the calculated ratios given by these three expressions. Results are given for fifteen different pairs of diodes, which were all the possible combinations of six diodes that had V_{20} and V_{100} values extending through the whole range of values exhibited by production. The values are given in Table 2. The combinations of diodes in Table 1 are arranged so that the smallest differences in V_{100} are on the left hand and the largest on the right. Diodes E and F were early samples with V_{100} values lying above the later production spread shown by Fig. 2.

TABLE 2

Measured values of V_{20} and V_{100} of six rectifier diodes

Diode	A	B	C	D	E	F	
V_{20} value	0·90	0·91	0·91	0·94	0·94	0·98	V
V_{100} value	1·15	1·19	1·22	1·27	1·31	1·38	V

It can be seen from Table 1 that the calculated ratios differ according to the equation used. Thus, for d.c. conditions, the values obtained by the use of Eq(13), given in line (a), differ from the Eq(20) values in line (b). Similarly, lines (c) and (d) show differences for six-phase operation. It has been assumed, in the calculations, that both diodes have the same junction temperature. This assumption is justified if the diodes are mounted on one heatsink.

It should be noted that the accuracy of the calculations is dependent on the accuracy with which the diode voltage drop V_i is measured. An error of ±1% in the measurement of V_i will produce a difference of about ±8% in the calculated current ratio.

MEASUREMENT OF CURRENT DIFFERENCE

The same fifteen combinations of rectifier diode were used for practical measurements under d.c., six-phase, and half-wave conditions. The measurements, given in Table 1, were made with the devices mounted either (i) each diode on its own heatsink (lines f and i), or (ii) both diodes on one heatsink, with 100mm spacing between diode centres (line g), or (iii) both diodes on one heatsink with 40mm spacing between diode centres (lines h, j, and k). In all instances, the diode nuts were tightened with a torque of 150kg.cm to ensure good thermal contact.

The following measurements were made on each diode:

Average current i_{av}

at 0, 15, and 30 minutes after switch-on

Mounting base temperature T_{mb}

at 0, 15, and 30 minutes after switch-on.

The readings at 30 minutes can be regarded as steady-state values, and these are quoted in Table 1.

A resistance of 0·2mΩ was connected in series with the diode for the purpose of current measurement. The contact resistance in series with each diode was 0·05mΩ. The influence of these small additional resistances was very slight (see *Series Resistance*, page 84).

Comparison of Results

It will be seen from Table 1 that the best agreement between calculated and measured values of the current ratio under d.c. conditions is obtained when Eq(13) is used for the calculations; if the measured ratios in lines (f), (g), and (h) of the table are compared with the calculated ratios in lines (a) and (b), it is seen that the Eq(13) value of line (a) is the closer to the average of lines (f), (g), and (h). The marked discrepancies between lines (a) and (f), as shown, for example, by the pairs A-F, C-E, and B-F, are caused by temperature divergences that occur when the diodes are mounted on separate heatsinks.

For six-phase conditions, however, Eq(20) gives better agreement, as may be seen from a comparison of lines (c) and (d) with the average of lines (i) and (j).

The calculated ratios for half-wave conditions, obtained by means of Eq(18), and given in line (e), are reasonably close to the measured ratios of line (k).

A further comparison of calculated and measured values of the $i_{1(av)}/i_{2(av)}$ ratio is provided by Fig. 9, for d.c. conditions, with the diodes mounted on individual heatsinks. The values calculated by means of Eq(13) are plotted on the vertical scale. These are the values from line (a) of Table 1. On the horizontal scale are the measured values of the ratio. For each of the fifteen pairs of diodes, two values are given: first, that observed immediately after switch-on, and secondly, the steady-state value

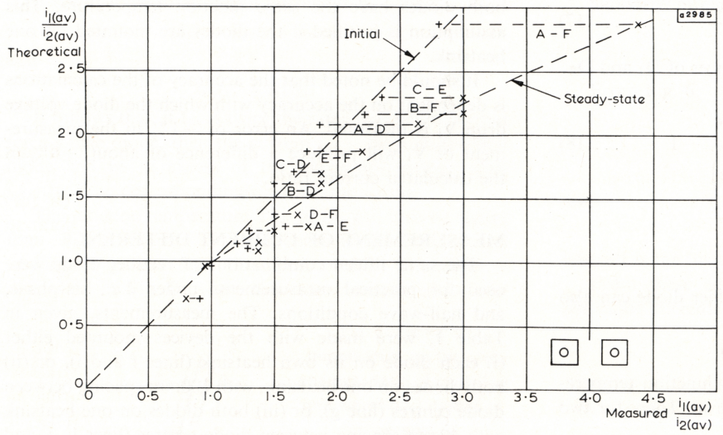

Fig. 9—Measured current ratio versus calculated value, under d.c. conditions, showing the effect of temperature divergence when separate heatsinks are used. A-F etc. indicate diode pairs

+immediately after switch-on
×steady-state values after 30 minutes

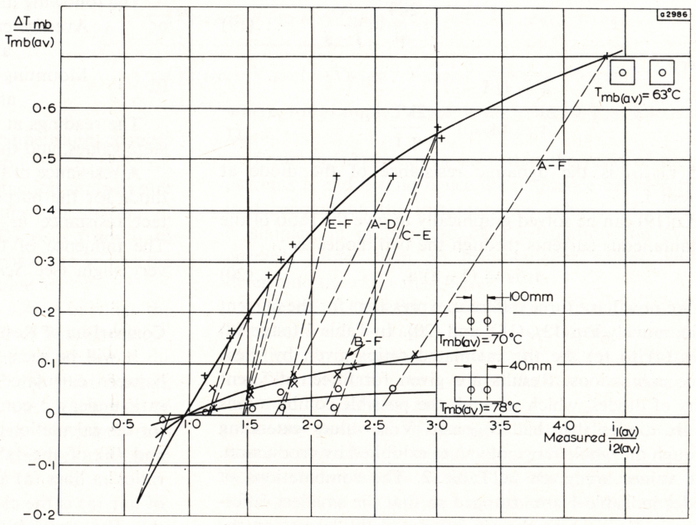

Fig. 10—Measured current ratio versus temperature rise, under d.c. conditions after 30 minutes, showing effect of heatsink sharing and of diode spacing. A-F etc. indicate diode pairs

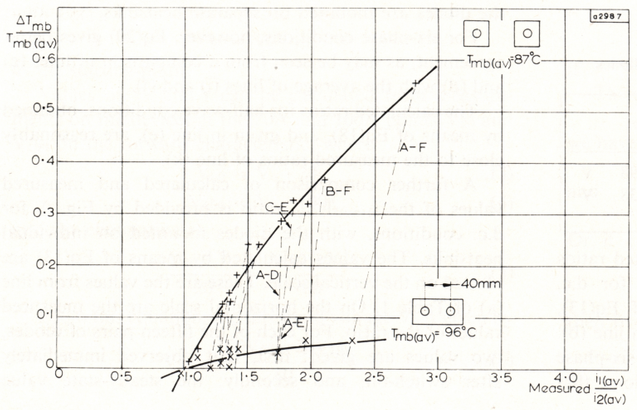

Fig. 11—Measured current ratio versus temperature rise, under six-phase conditions after 30 minutes, showing effect of heatsink sharing. A-F etc. indicate diode pairs

observed after a 30-minute run. These latter values are those given in line (f) of Table 1. It will be seen that the values observed immediately after switch-on agree well with the calculated values; while the steady-state values can be considerably higher than the calculated values, because of the effect of the divergence in junction temperature that occurs when separate heatsinks are used.

The advantage of mounting both diodes on one heatsink is shown in Fig. 10 for d.c. operation. The current ratios observed after a 30-minute run are plotted against the ratio $\Delta T_{mb}/T_{mb(av)}$ for three different heatsink arrangements. The three curves correspond to lines (f), (g), and (h) of Table 1. In the graph,

$$\Delta T_{mb} = T_{mb(1)} - T_{mb(2)}$$

and

$$T_{mb(av)} = \frac{T_{mb(1)} + T_{mb(2)}}{2}$$

where $T_{mb(1)}$ and $T_{mb(2)}$ are the mounting base temperatures of the two rectifier diodes.

It is obvious, from Fig. 10, that a much greater current difference occurs when the two diodes are mounted on separate heatsinks; and that the difference is much reduced when both diodes are on one heatsink and when the spacing between them is kept to a minimum.

Similar results for six-phase operation are shown in Fig. 11, where the curves correspond to lines (i) and (j) of Table 1.

REMEDIAL MEASURES

The results that have been presented in Table 1 and Figs. 9, 10, and 11, indicate that large differences in current can occur between two rectifier diodes connected in parallel, and that steps must be taken to keep both current and temperature within the device ratings.

The value of one remedial measure – the reduction of temperature difference by the sharing of a common heatsink – has already been demonstrated. However, this method is only one of several possibilities. Six methods, including heatsink-sharing ('thermal coupling') will now be discussed and assessed. The methods are:

(i) selection of diodes for minimum spread of characteristics
(ii) temperature derating, by the use of larger heatsinks or increased air-cooling
(iii) thermal coupling
(iv) use of series resistors
(v) use of balancing transformers.
(vi) current derating, in which the total current is shared between an increased number of parallel diodes.

In practice, it may be desirable or necessary to combine two or more of these methods.

SELECTION OF DIODES

It is possible to limit the current difference by using diodes that have only a small difference between their forward characteristics. Thus, in Table 1 (page 88) the diode combinations that have a V_{100} difference less than, say, 70mV are seen to have small $i_{1(av)}/i_{2(av)}$ ratios; and, in Figs. 9, 10, and 11, they are not among the pairs that give the least favourable performances.

The production of, say, the BYZ14 could be divided into two or three sub-types with V_{100} differences less than, say, 70mV; and, in any one rectifier installation, diodes from only one of these sub-types would be used.

The use of selection has the advantage that the diodes can be operated with little or no current derating. In the ideal case, diodes with *no* differences between their forward characteristics would be used, and neither derating nor any other measure would be required.

Selection, however, is troublesome to the rectifier user. To the rectifier manufacturer, it presents economic and production problems of some magnitude. Thus, in place of x types of rectifier diode, he would have to provide $3x$ or more types. And, in any event, there are unavoidable shifts in the mean value of any characteristic during an extended production run; so that it would sometimes be impossible to supply diodes of the sub-types that lie at the ends of the total spread of the original diode type.

For these reasons, it is not generally desirable to resort to selection.

TEMPERATURE DERATING

If the cooling system is designed as for optimum performance of single diodes, the unequal current-sharing between two or more diodes will take the 'best' diodes above their maximum temperature rating. If, however, the system is designed for a θ_{mb-amb} that is 25% below the published nominal value, then the margin will ensure that the rated junction temperature of the best diodes will not be exceeded. The effect of this temperature derating will be equivalent to that of a current derating of $0{\cdot}8 + (0{\cdot}2/n)$, as recommended on page 86.

With this form of protection, the maximum current obtainable is the nominal rated current of each diode, multiplied by the number of diodes; and the size of the installation is not increased by any extra diodes. However, the larger heatsinks required, or the increased forced-air cooling, may not be acceptable in some installations.

THERMAL COUPLING

It has already been shown, in Table 1 and Figs. 9, 10, and 11, that the sharing of heatsinks and the reduction of the distance between diode centres has a favourable effect. The mounting base temperatures will be more or less equalised, and the junction temperature of the best diode will be kept down. The reduced difference in junction temperatures will counteract the divergence of forward characteristics, so that current differences, as already seen, will be considerably reduced.

The value of θ_{mb-amb} for a single heatsink carrying n diodes must be the n^{th} fraction of the nominal θ_{mb-amb} required for a single diode.

Thermal coupling, in combination with other methods of protection, is strongly recommended. Care must be taken, however, in the calculation of the heatsink (Ref. 3) to ensure that the diode spacing is not so small that the efficiency of the heatsink is seriously impaired.

SERIES RESISTANCE

Current differences can be reduced by the connection of equal resistances in series with each diode. The differing internal resistances of the diodes will then form smaller parts of the total resistance of each path, and the currents will therefore show less divergence. The effect is illustrated

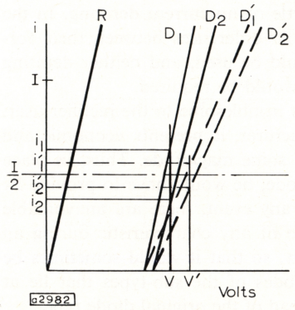

Fig. 12—Division of current with and without series resistance

in Fig. 12, where the addition of a series resistance R in the circuit of diode D_1 shifts the forward characteristic from D_1 to D_1'; and similarly with diode D_2. If the added resistance is several times the internal resistance of the diode, then substantial equalisation of currents can be achieved, at the cost, however, of increased losses.

The determination of the value of series resistance is based on two principles:

(i) the dissipation must be equal in each diode,

(ii) the current through the best diode must not exceed the maximum published rating.

Equal Dissipation

Consider two diodes in parallel. The dissipation of a diode in a six-phase star circuit is

$$W_6 = \frac{i_{pk}}{6}V_o + \frac{i_{pk}^2}{6}r \qquad \ldots(21)$$

and in a three-phase star circuit it is

$$W_3 = \frac{i_{pk}}{3}V_o + \frac{i_{pk}^2}{3}r. \qquad \ldots(22)$$

In these two configurations, the condition for equal dissipation in two parallel diodes is

$$i_{pk(1)}.V_{o(1)}+i_{pk(1)}^2.r_1 = i_{pk(2)}.V_{o(2)}+i_{pk(2)}^2.r_2. \qquad \ldots(23)$$

Furthermore,

$$I_{pk} = i_{pk(1)}+i_{pk(2)}$$

and

$$V_{pk} = V_{pk(1)} = V_{(pk)2}$$

so that

$$V_{pk(1)} = V_{o(1)}+i_{pk(1)}(r_1+R) \qquad \ldots(24)$$

and

$$V_{pk(2)} = V_{o(2)}+i_{pk(2)}(r_2+R), \qquad \ldots(25)$$

where R is the series resistance.

It can be shown that

$$R = \frac{I_{pk}.r_2+i_{pk(1)}(r_1+r_2)+V_{o(2)}-V_{o(1)}}{2i_{pk(1)}-I_{pk}}. \qquad \ldots(26)$$

When more than two diodes are connected in parallel account must be taken of the spread of forward characteristics shown in Fig. 2. The calculations required are extensive: but, for practical purposes, satisfactory equalisation of diode temperatures is obtained if the value of R is chosen so that, at the maximum rated peak forward current, the peak voltage drop across the resistor is 1·5V. This procedure is adequate not only for three-phase and six-phase configurations, but for all types of circuit.

Diode Current equal to Rated Values

For n diodes in parallel, with j being some number intermediate between 1 and n,

$$V_{pk} = i_{pk(1)}(R+r_1)+V_{o(1)} = i_j(R+r_j)+V_{o(j)} = \ldots\ldots = i_{pk(n)}(R+r_n)+V_{o(n)} \qquad \ldots(27)$$

and

$$I_{pk} = \sum_{j=1}^{j=n} i_{pk(j)}. \qquad \ldots(28)$$

It can be shown that

$$I_{pk} = i_{pk(max)} + \frac{i_{pk(max)}(R+r_1)-(V_{o(2)}-V_{o(1)})}{R+r_2}(n-1) \qquad \ldots(29)$$

where $i_{pk(max)}$ is the maximum peak current rating of the diode.

Theoretical derating factors for $i_{pk(max)}$ are given for various values of series resistance R in Table 3, for the BYZ14. The theoretical value of I_{pk} is the published value of $i_{pk(max)}$ multiplied by the factor given in the centre column.

TABLE 3

Derating Factors for $i_{pk(max)}$

R (mΩ) ±5%	I_{pk} (A) calculated	I_{pk} (A) practical
	$i_{pk(max)}\times$	$i_{pk(max)}\times$
0	0·65n+0·35	0·80n+0·20
1·5	0·74n+0·26	0·85n+0·15
5·0	0·83n+0·17	0·90n+0·10
7·5	0·87n+0·13	0·93n+0·07
10·0	0·89n+0·11	0·95n+0·05

The factors in the third column allow for the spread in forward characteristics from diode to diode. These are the factors that should be used (see *Current Derating*).

When each BYZ14 is protected by a fuse (with a minimum rating of $1{\cdot}15\times i_{rms(nom)}$) it is reasonable to base the I_{pk} calculation on a series resistance of about 1·5mΩ. A derating factor of $d = 0{\cdot}85+(0{\cdot}15/n)$ is then adequate.

The contact resistances of the rectifier paths must be as nearly equal as possible. The worst case is when there is a low contact resistance in series with the best diode, and a high contact resistance in series with the worst diode. These conditions give the greatest accentuation of the current difference.

The series resistance method of protection allows less severe current derating of the rectifier diodes than that recommended on page 86; but there is an increase in losses, and the ±5% high-wattage resistors and their mountings add significantly to the cost of the installation.

BALANCING TRANSFORMERS

The principle of the balancing transformer is shown in Fig. 13. Each of the two parallel diodes has in series with it a transformer winding, both windings being on the same

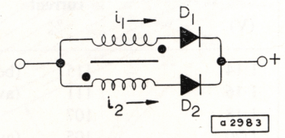

Fig. 13—Two parallel rectifier diodes with balancing transformer

core. If D_1 is the best diode and D_2 the worst, then $V_{o(1)}<V_{o(2)}$, and D_1 will conduct earlier in the positive half-cycle than D_2. The current i_1, flowing through the winding associated with D_1, will induce a current in the other winding, thus forcing D_2 to conduct. The current i_2 will set up an opposing field, and i_1 will be reduced. This interaction will tend to correct the unbalance of the diode currents.

For the calculation of the inductance of each winding, the following empirical formula may be used:

$$L = \frac{1}{\omega.i_{pk(nom)}\delta} \qquad \ldots(30)$$

where δ is

$$\frac{i_1-i_2}{\frac{1}{2}(i_1+i_2)}.$$

If $\delta \leqslant 0{\cdot}05$ and f = 50c/s, then

$$L = \frac{63{\cdot}5}{i_{pk(nom)}}\text{mH} \qquad \ldots(31)$$

and no further derating is required.

When more than two diodes are connected in parallel, a 'closed chain' arrangement is recommended, as shown in Fig. 14. If, in this circuit, any one of n diodes is disconnected by the blowing of a fuse, the circuit continues

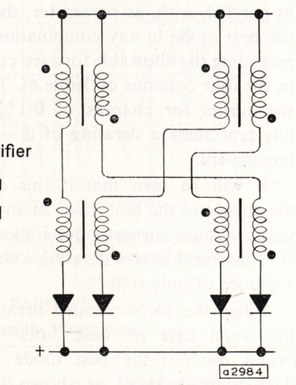

Fig. 14—Four parallel rectifier diodes with balancing transformer in 'closed chain'

to provide current-sharing; but the remaining diodes will, of course, be overloaded by the $(n-1)^{th}$ part of the current of the disconnected diode.

The use of balancing transformers allows the diodes to be used without any current derating, and the added losses are small. The disadvantages are the cost of the transformers, the increase in the bulk of the installation, and the switching transients that are produced.

CURRENT DERATING

It is unlikely that, in any installation, one 'best' diode (Fig. 2) will be connected in parallel with one or several 'worst' diodes. However, as Table 1 and the associated graphs have shown, diodes with *less* than the maximum characteristic difference can run with unacceptably large current differences; and the best diode of those used in an installation is likely to be overrun.

Current-sharing can be improved by the techniques that have already been discussed; but, unless a suitable balancing transformer or a sufficiently large series resistor is used, some measure of current derating must be employed to ensure that the best diode of the group operates at the maximum current rating, and all the other diodes at less than the maximum rating.

Two ways of achieving this derating are possible: either to reduce the total current that is taken from the installation, or to share the current between a larger number of parallel diodes. At the design stage of the installation, of course, these two approaches amount to the same thing: the installation must be designed so that the total current and the number of parallel diodes are such that the best diode in the worst probable combination of diodes will run at the maximum current rating of the type.

The third section of Table 1 (page 88) gives the calculated derating factors that would ensure the safe running of each of the fifteen combinations. It will be seen that the diode combinations with the largest differences in their forward characteristics (namely, those toward the right of the table) have the most severe derating factors. In the worst cases, it is necessary to reduce the current to about 60% of its original value. These deratings have been calculated in the following way.

Let the measured ratio $i_{1(av)}/i_{2(av)} = y$ for a particular diode pair.

The maximum average current rating of each BYZ14 diode is 40A, so that the average total current that may be conducted is $2\times40 = 80$A. The total current that may be conducted in practice is $40\left(1+\frac{1}{y}\right)$A; therefore the derating factor is

$$d = \frac{40\left(1+\frac{1}{y}\right)}{80}.$$

As an example, the required derating for the pair A-F, under half-wave conditions, is given by:

$$y = i_{1(av)}/i_{2(av)} = 2{\cdot}64$$

from line (k) of Table 1.

$I_{1(av)} = 40$A

$I_{2(av)} = I_{1(av)}/y = 40/2{\cdot}64 = 15{\cdot}1$A

$I_{total} = I_{1(av)}+I_{2(av)} = 40+15{\cdot}1 = 55{\cdot}1$A

For this total current to flow, the nominal rating of 80A must be derated by

$$d = 55{\cdot}1/80 = 0{\cdot}69$$

which is the value given in line (q) of Table 1.

Determination of Practical Derating Factor

The spreads of forward voltage of the BYZ14 at 10A and 100A (under pulse conditions) are shown in Fig. 2 (page 78). The total production can be divided into four groups, on the basis of the forward voltage V_{100} at 100A forward current. Table 4 shows the relative numbers of diodes in each group.

TABLE 4
Distribution of V_{100} for BYZ14

	V_{100} range (V)	Percentage of Production (%)
I	1·14 to 1·18	19
II	1·18 to 1·22	46
III	1·22 to 1·26	24
IV	1·26 to 1·30	11

Since the published maximum dissipation rating is derived from the characteristic of the worst diodes (with $V_{100} = 1{\cdot}30$V), it is obvious that the best diode (with $V_{100} = 1{\cdot}14$V) can carry a greater forward current before it reaches the maximum dissipation rating.

The dissipation of a diode is given by

$$P = i_{av}.V_o + i_{rms}^2.r. \qquad \ldots(32)$$

In a six-phase rectifier circuit the dissipation of each diode is

$$P_6 = \frac{I_{pk}}{6}V_o + \frac{I_{pk}^2}{6}r. \qquad \ldots(33)$$

The worst BYZ14 is seen, from Fig. 2, to have $V_{100} = 1{\cdot}3$V and $V_{10} \simeq 0{\cdot}9$V. From these two measured points the values of V_o and r can be calculated.

Thus $$V_o = \frac{10V_{10} - V_{100}}{9} = 0{\cdot}855\text{V}$$

and $$r = \frac{V_{100} - V_{10}}{90} = 4{\cdot}45 \times 10^{-3}\Omega.$$

The published value of i_{av} for each BYZ14 in a six-phase rectifier circuit is $192/6 = 32$A, for a maximum rated peak forward current of 200A. So, for the worst diode, the maximum forward dissipation is, from Eq(33), 58W (the published value includes about 2W reverse dissipation).

For the best diode, $V_{100} = 1{\cdot}14$V and $V_{10} = 0{\cdot}85$V, so that $V_o = 0{\cdot}819$V and $r = 3{\cdot}22 \times 10^{-3}\Omega$.

Substitution of these values shows that, for a maximum forward dissipation of 58W, the peak forward current is about 230A—which is 15% above that allowable for the worst diode (that is, above the published maximum peak forward current).

Similar calculations for diodes intermediate between the best and worst provide the maximum allowable current values given in Table 5.

It is now possible to calculate the maximum allowable currents for various combinations of diodes. These are given in Table 6 and Fig. 15.

Column A applies if the diodes used come from all four groups; column B if there are no diodes from Group I; column C if there are no diodes from Groups I or II; and column D if all the diodes come from Group IV (that is, the worst group). Thus, if diodes from all four groups are paralleled, then those from Group I can run at 111% of the nominal current value while those from Group III must be derated by 8% and those from Group IV by 15%.

TABLE 5
Allowable Forward Current

V_{100} (V)	Percentage of nominal maximum current %	
1·14	115	(best diode)
1·16	111	(average diode of group I)
1·18	107	
1·20	105	(average diode of group II)
1·22	103	
1·24	102	(average diode of group III)
1·26	101	
1·28	100	(average diode of group IV)
1·30	100	(worst diode)

TABLE 6
Allowable Forward Current

Group	Percentage of nominal current A	B	C	D
I	111	—	—	—
II	100	105	—	—
III	92	96	102	—
IV	85	89	94	100

Fig. 16 (based on Fig. 2) shows the current derating factor d as a function of the number of diodes n connected in parallel, with, as parameter, the chance of overloading the best diode in any combination (that is, the chance of exceeding the allowable forward currents that are indicated in the four columns of Table 6). The two broken lines are the curves for chances of 0·1% and 0·01%. The full line represents a derating of $d = 0{\cdot}8 + (0{\cdot}2/n)$, which we recommend.

It will be seen that if this derating factor is used, the chance of the best diode in any combination exceeding the maximum current value indicated in Table 6 is 0·1%. A rather more severe derating would be required to ensure a chance of only 0·01%.

When the recommended derating is applied, then, in the worst case (a 'best diode' paralleled with (n−1) 'worst diodes') the best diode will have a maximum dissipation overload as shown in Table 7 for various values of n.

Dissipation overloads of these magnitudes will give thermal runaway only if the diode has the maximum published value of $\theta_{j\text{-case}}$, which again is unlikely. In any event, thermal stability will be substantially improved if the recommendation to use a shared heatsink is followed.

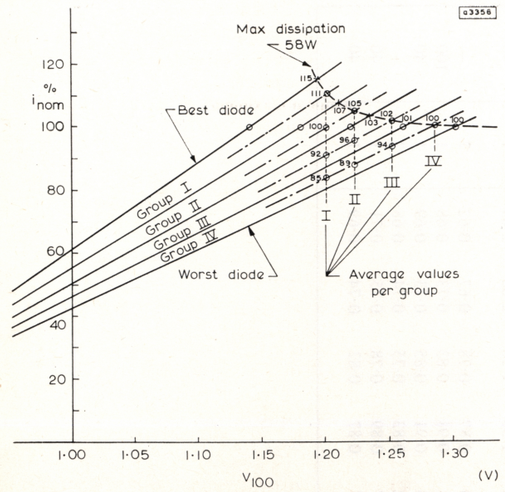

Fig. 15—Maximum allowable current per diode for various values of V_{100}

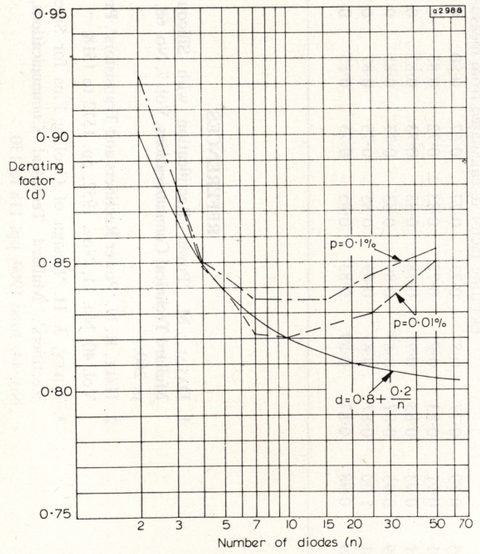

Fig. 16—Derating factors (d) for 2 to 60 diodes in parallel, for 0·1% and 0·01% chance (p) of overloading the best diode

TABLE 7
Overload in Worst Case

Number (n) in parallel	Dissipation overload of best diode (%)
5	0
10	4
50	7·5

To check the calculations, ten unselected BYZ14 have been connected in parallel and their currents measured. It was found that a current derating of 0·85 was sufficient to keep the best diode within ratings. This value is less severe than the calculated value which, for ten diodes, is (from the full line in Fig. 16), $0{\cdot}8 + (0{\cdot}2/10) = 0{\cdot}82$. The use of the calculated value has thus provided a margin of safety in this example; and the recommended acceptance of a 0·01% chance of overload appears to be justified.

This form of diode protection – by current derating – has the advantage that it does not need supplementing by any other protection method (but thermal coupling should also be used to give additional protection). However, there is the obvious disadvantage that more diodes (and therefore a larger installation) will be necessary for any particular required total current.

SURGE CHARACTERISTICS

Equalisation of diode operation has been discussed in terms of average currents. However, diodes with differing forward characteristics will also share surge currents unequally. Similar considerations apply to surge currents as to average currents.

Published surge current ratings are based on the characteristics of the worst diode, since this is the diode that will first reach the maximum dissipation. A better diode will reach this limit at higher currents.

Measurements have shown that current-sharing at these high surge currents is somewhat better than at average currents. Satisfactory protection will be given if the fuse in series with each diode is rated at $1{\cdot}15 \times i_{rms(nom)}$.

RECOMMENDATIONS

Which method, or combination of methods, is used is determined mainly by cost and by the required reliability of the installation. The following guidance is offered:

(1) If diodes are connected in parallel without any additional circuit elements, then either of the following deratings should be used:
  (i) average current to $0{\cdot}8 + (0{\cdot}2/n)$ of the nominal published value or
  (ii) thermal resistance of heatsink to 75% of the nominal required value.

(2) Thermal coupling of diodes is strongly recommended, whatever other measures are employed. With n diodes, the thermal resistance of the shared heatsink should be the n^{th} fraction of the value required for one diode.

(3) A fuse in series with a diode acts as a small series resistance, and improves current-sharing. Current derating to $0{\cdot}85 + (0{\cdot}15/n)$ is then sufficient.

(4) No derating is necessary when using either
  (i) a balancing transformer with $L = 20/(\omega . i_{pk(nom)})$H or
  (ii) a ±5% series resistor, for each diode, such that the peak voltage drop across the resistor is 1·5V at nominal peak current.

(5) The electrical and mechanical layout must be as symmetrical as possible.

(6) Selection of diodes may be resorted to; but, in general, it is more convenient and economic to use other methods.

TABLE 1

Current Spread and Current Derating Factors for Fifteen BYZ14 Pairs

Circuit configuration	Formula	Diode combination and V_{100} difference in mV														Heatsink configuration	
		B-C 30	A-B 40	D-E 40	C-D 50	A-C 70	E-F 70	B-D 80	C-E 90	D-F 110	A-D 120	B-E 120	C-F 160	A-E 160	B-F 190	A-F 230	Heat-sinks	Diode spacing (mm)
		Calculated ratio $i_{1(av)}/i_{2(av)}$															
a D.C.	13	0·94	1·25	0·71	1·69	1·15	1·85	1·62	2·30	1·38	2·08	1·06	1·12	1·28	2·18	2·83	—	—
b D.C.	20	1·00	1·10	0·85	1·28	1·09	1·54	1·29	1·73	1·35	1·43	1·09	1·07	1·20	1·78	1·96	—	—
c Six-phase	13	0·91	1·20	0·57	1·91	1·07	3·70	1·78	4·62	2·04	2·21	0·94	1·03	1·10	4·38	6·45	—	—
d Six-phase	20	1·11	1·16	1·07	1·17	1·28	1·17	1·31	1·50	1·27	1·52	1·38	1·24	1·60	1·68	1·95	—	—
e Half-wave	18	1·28	1·16	1·30	1·23	1·27	1·41	1·28	1·69	1·37	1·49	1·51	1·30	1·56	1·78	2·10	—	—
		Measured ratio $i_{(av)}/i_{2(av)}$ under steady-state conditions															
f D.C.		0·95	1·50	0·64	1·86	1·35	2·20	1·86	3·00	1·67	2·64	1·16	1·35	1·76	3·00	4·33	2	—
g D.C.		0·95	1·22	0·82	1·50	1·22	1·86	1·50	2·33	1·50	1·86	1·22	1·22	1·50	2·20	2·81	1	100
h D.C.		1·00	1·22	0·86	1·50	1·22	1·76	1·50	2·20	1·50	1·76	1·16	1·22	1·43	2·20	2·64	1	40
i Six-phase		1·05	1·29	1·10	1·35	1·35	1·29	1·50	1·85	1·42	1·76	1·58	1·50	1·96	2·08	2·81	2	—
j Six-phase		1·10	1·22	1·00	1·35	1·35	1·29	1·42	1·76	1·35	1·76	1·35	1·29	1·76	1·96	2·33	1	40
k Half-wave		1·10	1·29	0·95	1·35	1·29	1·50	1·42	1·96	1·42	1·76	1·35	1·35	1·58	2·08	2·64	1	40
		Derating factor d, calculated from measurements															
l D.C.		0·98	0·83	0·89	0·77	0·87	0·73	0·77	0·67	0·80	0·69	0·93	0·87	0·78	0·67	0·62	2	—
m D.C.		0·98	0·91	0·91	0·83	0·91	0·77	0·83	0·72	0·83	0·77	0·81	0·91	0·83	0·73	0·68	1	100
n D.C.		1·00	0·91	0·93	0·83	0·91	0·78	0·83	0·73	0·83	0·78	0·93	0·91	0·85	0·73	0·69	1	40
o Six-phase		0·98	0·89	0·95	0·87	0·87	0·89	0·83	0·77	0·85	0·78	0·82	0·83	0·75	0·74	0·68	2	—
p Six-phase		0·95	0·91	1·00	0·87	0·87	0·89	0·85	0·75	0·87	0·78	0·87	0·89	0·78	0·75	0·71	1	40
q Half-wave		0·95	0·89	0·98	0·87	0·89	0·83	0·85	0·75	0·85	0·70	0·87	0·87	0·82	0·74	0·69	1	40

REFERENCES

1. DAYAL, M. 'Power Rectification with Silicon Diodes', **Mullard Technical Communications,** Vol. 7, No. 68, Jan. 1964, p. 260.
2. HALL, R. N. 'Power Rectifiers and Transistors'. **Proc. I.R.E.,** Vol. 40, No. 11, Nov. 1952, pp. 1512 to 1518.
3. TULEY, J. H. 'Design of Cooling Fins for Silicon Power Rectifiers'. **Mullard Technical Communications,** Vol. 5, No. 44, June 1960, pp. 118 to 130.